

Finite hard-rod systems and their thermodynamic limit: Survey of methods and results

P. Kasperkovitz and J. Reisenberger

Institut für Theoretische Physik, Technische Universität Wien, Karlsplatz 13, A-1040 Wien, Austria

(Received 28 August 1984)

We consider N particles, each of mass m and diameter d , moving on a line and interacting via elastic collisions. The particles are enclosed by a freely movable, massless box of length L . The center of mass is assumed to be at rest. We state results on ergodic properties (equivalence of time and ensemble averages, approach to equilibrium) and outline their proof. We also list exact expressions for some expectation values (pair distribution function, pressure, collision frequency, no-collision probability, velocity autocorrelation function) obtained for fixed parameters N, m, d, L and three kinds of ensembles (smallest stationary, microcanonical, canonical) and discuss their thermodynamic limits. The derivation of these results, based on a generalization of a method already used for small systems ($N \leq 3$), is illustrated here with specific examples.

I. INTRODUCTION

In all fields of physics, exactly soluble problems are the exception rather than the rule. Nevertheless they are studied again and again, and the research for new ones persists. This happens for at least two reasons: Firstly, some of these problems lie at the heart of every theory, making one hope that the theory will eventually apply to the case it was originally intended to model. Secondly, these problems may be used to test calculation schemes developed at least to obtain approximate solutions of similar problems which are more complicated but also more interesting.

If one is interested in the properties of a real dynamical system, one usually has to choose an oversimplified model to arrive at well-defined, solvable mathematical problems. In this simplification, contact with reality is greatly diminished since usually only a few essential features of the original system are to be correctly described by the model. This is well illustrated by the system considered here: a finite number of particles enclosed by a box, moving on a line, and undergoing elastic collisions. This might be viewed as a model of an abacus, but with regard to real gases or fluids one can at best expect some qualitative similarity. It is therefore rather questions of principle which make this system an interesting object of investigation. The second reason to study this model seems to be less stringent in the present case. Although there are several different (or differently looking) methods to compute a physical quantity of interest, they all turn out to be especially adapted to the problem at hand, i.e., to one-dimensional motion and elastic collisions.

The questions of principle considered here fall into two categories. The first group is concerned with dynamical properties of the system and the two main questions read, "Can time averages be replaced by ensemble averages?" and, "Does an initial distribution in phase space evolve toward an equilibrium distribution?" In the following we will answer these questions for finite systems. The second group questions may be summed up as, "What can we learn about large systems from studying small ones?" To

find an answer to this question we calculate the expectation values of five observables (pair distribution, pressure, collision frequency, no-collision probability, velocity autocorrelation function) for three ensembles (smallest stationary, microcanonical, canonical). Having obtained the result for a finite system with given number of particles, size, etc., we take the thermodynamic limit (whenever this makes sense). Knowing the members of the sequence explicitly, one can see how fast (or slowly) an expectation value converges to its thermodynamic limit and whence apparent qualitative differences between finite and infinite systems originate.

The method that we used to discuss the topics mentioned above differs from those used in other similar investigations. Until now this method has been employed only for systems corresponding to the simplest system considered here ($N=2$); therefore its generalization and application to the general N -particle system deserve some explanation. Because of this—and since emphasis is put onto the pedagogic aspects of the model—it seemed to be appropriate to start with a survey of methods and results before entering into the details of the calculation. This is the principal purpose of the present paper, which is organized as follows: In Sec. II we show how our results are related to those of previous investigations of similar systems. In Secs. III and IV the two- and three-particle systems are studied in detail since one can learn from studying these simpler systems how best to treat the N -particle system. Results for general N are listed in Sec. V, and their thermodynamic limits are discussed in Sec. VI. Finally, Sec. VII contains our conclusions and a brief comment on possible generalizations of the model considered here. A detailed derivation of our results will be given elsewhere.

II. COMPARISON OF OUR RESULTS WITH THOSE OF PREVIOUS INVESTIGATIONS

To compare our work with that of others, we have to start by defining the system. We consider N particles, each of mass m and diameter d , moving on a line and in-

interacting through elastic collisions. The particles are assumed to be enclosed by a freely movable, massless box of length L . This device makes the first and the last particle collide like nearest neighbors, and defines the volume of the "hard-rod gas." As is obvious from Fig. 1, this system is essentially equivalent to a ring system, the only difference being the position of the center of mass (c.m.). In the linear system this variable is uniquely defined, in the ring system it is defined only modulo L . Under a collision two particles exchange their velocities. Hence the total momentum is a constant of motion and the c.m. moves uniformly along the line. This does not affect the relative motion of the particles which is the same for both the linear and the ring system. Labeling the particles by $i = 1, \dots, N$ we therefore eliminate the trivial part of the evolution by requiring that

$$\sum_{i=1}^N x_i = 0, \quad \sum_{i=1}^N v_i = 0, \quad (1)$$

for all times. This reduces the degrees of freedom from N to $N - 1$ but makes it more difficult to compare our results with others since, e.g., factorizable distributions of initial conditions are ruled out by (1). However, observing (1) throughout the following allows us to see what effects are entirely due to the relative motion. Moreover, if a motion of the c.m. is admitted or even desired for some reason the result obtained here can be easily modified because the internal evolution does not interfere with the motion of the c.m.

Since the particles are not allowed to penetrate through each other in this model the ordering in the beginning, say $x_1 < x_2 < \dots < x_N$, remains the same for all later times. This means that it is possible to distinguish the particles by their order. It has been claimed¹⁻³ that if the particles are indistinguishable they may be treated as free particles passing each other without collisions. This, however, is not true because one can observe a collision and count it without knowing the numbers of the colliding particles. Therefore the ring systems considered by Frisch^{1,2} differ essentially from those considered here since there all particles are assumed to move freely around the circle. All similarities in his and our results originate solely from the confinement of the particles. It also has been claimed⁴ that the system may be treated as a collection of free particles if the diameter d shrinks to zero (and phase-space functions symmetric in the positions and velocities of the particles are considered⁵). If this would really make the particles indistinguishable one would be unable to say whether two particles, after having arrived at the same position, have passed through each other or have been reflected. Hence the dynamics of such a system is undefined unless a convention is made about what happens in such a situation. It makes a difference whether such an event is counted as collision or not and this shows up in the way the (symmetrical) phase-space functions measuring the pressure, the collision frequency, etc. are defined and interpreted.

The finite systems discussed in the literature are either ring systems or linear systems with fixed walls. It should be noted that the constraint (1) makes our two-particle system mathematically completely equivalent to the one-

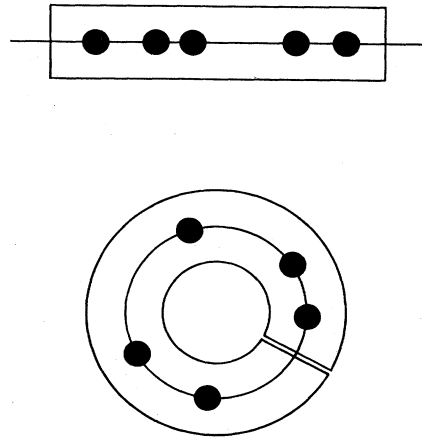


FIG. 1. Linear system and ring system.

particle system with fixed walls. This system has been investigated by Born⁶ and Deutch *et al.*,⁷ its generalization to N noninteracting particles by Teramoto and Suzuki⁸ and by Nossal,⁹ and to three dimensions by Hobson and Loomis.¹⁰ Fixed-wall systems with more than one impenetrable particle have been considered by Tonks,¹¹ Leff and Coopersmith,¹² Lebowitz and Sykes,¹³ and Evans.¹⁴ Evans noticed that the fixed-wall system is equivalent to a ring system of double size, if the initial states of this system (and hence all the following ones) are suitably restricted. Evans also studied the ring system as did Jepsen¹⁵ some time before in his fundamental paper on the hard-rod gas. As pointed out before this system is completely equivalent to ours up to the constraint (1). If the size of the system increases one would expect the influence of the boundary conditions to decrease, becoming finally completely irrelevant in the limit of an infinite system. Such a system has been considered by Zernike and Prins¹⁶ already in 1927. Of the more recent papers on infinite hard-rod system (Refs. 17-22) the one of Lebowitz and Percus¹⁷ is most important for the problems considered here.

Once the dynamics of the system is defined, one may ask whether it is ergodic or not. A closed finite system is said to be ergodic if for almost all initial states the time average of a phase-space function equals its average over the energy surface containing the initial state.²³ None of the finite systems mentioned above meets this condition because impenetrable particles remain ordered and colliding particles do only exchange their velocities. A permutation of the particles, which would leave the total energy invariant, can never result from the evolution in time. Hence an orbit in phase space is confined to one of the $N!$ disjoint parts into which the energy surface decomposes. This argument against ergodicity could be invalidated by fixing a certain order once for ever. But for $N > 2$ the part of the energy surface filled by an orbit anyway incomparably smaller, i.e., of relative measure zero, because the set $\{v_{it}\} = \{v_{1t}, v_{2t}, \dots\}$ is conserved in time (for fixed walls $\{v_{it}\} \subset \{\pm v_{it}\}$). That finite hard-rod systems are not ergodic is well known, sometimes even mentioned explicitly.^{1,13}

Knowing that an orbit in phase space cannot leave a region characterized by the initial order, say $x_{i_1} < \dots < x_{i_N}$, and the set of initial velocities $\{v_{i_0}\}$ one would like to know whether the evolution is ergodic with respect to this

part of the energy surface. This is by definition, the case if the time average of the function $G(t) = g(X_t, V_t)$ equals the average of g over the set

$$\left\{ (X, V) \left| \begin{array}{l} X \text{ is a possible configuration;} \\ x_{P'1} < \dots < x_{P'N} \text{ for a fixed permutation } P: i \mapsto Pi; \\ v_{P'1} = v_{i_0}, \dots, v_{P'N} = v_{i_0} \text{ for some permutation } P': i \mapsto P'i. \end{array} \right. \right\}. \quad (2)$$

The equivalence of time and ensemble averages has been shown by Jepsen¹⁵ for noninteracting ring systems and functions of the form $g(X_t)$. He also stated without proof that this coincidence persists if the particles collide and general phase-space functions are considered. We supply a proof of this assertion for the systems considered here (c.m. at rest).

Closely related to the fact that the "smallest stationary ensemble" (2) is (for almost all sets of initial velocities v_{i_0}) the closure of one single orbit is the existence of recurrence times. This topic has been extensively discussed for ring systems, for the noninteracting one by Frisch^{1,2} and for the interacting one by Jepsen.¹⁵ We did not attempt to improve their results. We only want to point out that the geometrical method employed here simplifies the discussion of recurrence times for hard-rod systems considerably. For this method makes obvious which initial conditions lead to strictly periodic motions; it also shows clearly that in general the initial state is realized again not exactly but to any desired accuracy. Correlation functions of the form

$$G(t)H(t+\tau) = g(X_t, V_t)h(X_{t+\tau}, V_{t+\tau})$$

are therefore almost periodic and this is also true for the expectation values $\langle gh \rangle$ where $\langle \dots \rangle$ denotes either the time average or the average over the ensemble (2). Hence an irreversible decay of correlation functions can never be obtained from a time average alone but only by averaging over ensembles which, like the microcanonical and the canonical one, consist of an infinite number of smallest stationary ensembles.

The existence of recurrence times shows that a distribution function $\delta(X - X_t[X_0, V_0])\delta(V - V_t[X_0, V_0])$ representing the evolution $(X_0, V_0) \rightarrow (X_t, V_t)$ of a system whose initial state (X_0, V_0) is completely known, can never be approximated by a stationary function. However, if the initial condition is only known to be realized with a probability given by the distribution $f_0(X_0, V_0)$ it may happen that

$$\lim_{t \uparrow \infty} \int dX dV f_t(X, V)g(X, V) = \int dX dV f_{(\infty)}(X, V)g(X, V) \quad (3)$$

for sufficiently smooth functions g , where

$$f_t(X, V) = \int dX_0 dV_0 f_0(X_0, V_0) \delta(X - X_t[X_0, V_0]) \times \delta(V - V_t[X_0, V_0]) \quad (4)$$

and $f_{(\infty)}$ is a distribution uniquely defined by f_0 . In Eqs. (3), (4), and all the following ones which contain integrals each variable has to be integrated from $-\infty$ to $+\infty$ if not explicitly stated otherwise. Note that f vanishes if X does not belong to a bounded subset of \mathbb{R}^N . For one or more noninteracting particles moving between fixed walls examples of such an approach to equilibrium have been discussed by Born,⁶ Teramoto and Suzuki,⁸ and Frisch,² and Hobson and Loomis.¹⁰ Our discussion is more general in that we consider colliding particles and a whole class of initial distributions f_0 instead of a few examples. We give sufficient conditions for the existence of weak limits $f_0 \rightarrow f_{(\infty)}$, Eq. (3), and specify $f_{(\infty)}$ in terms of f_0 .

Another kind of limit we are especially interested in is the thermodynamic limit (TDL). There are very few examples (oscillator chains, spin systems, etc.) for which this limit has been actually performed considering the properties of all (or sufficiently many) members of the sequence. Mostly the term "thermodynamic limit" is merely used to fix some properties of the infinite system and to make plausible assumptions on its dynamics. For the hard-rod systems considered here the dynamics of the infinite system is in some respects simpler than that of a finite one, a fact which has been exploited by Lebowitz and Percus¹⁷ and Levitt¹⁹ and which is also perceivable in some of our results. A disadvantage of the infinite systems is that it is hard to guess how to modify a result obtained for such a system in case of a finite system. Consider for instance the pair distribution function $g_{\infty}(r)$, found by Zernike and Prins¹⁶ for $N = \infty$ and $d > 0$: It is zero for $0 \leq r < d$, then oscillates a few times with decreasing amplitude, finally tending to $\rho > 0$ for $r \uparrow \infty$. For a large but finite system one expects $g_N(r) \approx g_{\infty}(r)$ for small r ; but if r is sufficiently large $g_N(r) = 0$ since the distance of two particles is bounded in a finite system. Thus $g_N(r)$ has to decrease to zero but the function $g_{\infty}(r)$ does not give any hint how this should happen. As a second example consider the velocity autocorrelation function for a canonical ensemble. For the finite system Jepsen¹⁵ found an asymptotic decay proportional to t^{-3} , a result confirmed by Lebowitz and Percus¹⁷ who computed the shape of this function from $t=0$ up to the values considered by Jepsen. Later on Evans¹⁴ found that the velocity autocorrelation function for the canonical ensemble decays as $-t^2 \exp(-\alpha t^2)$, $\alpha = \alpha(N, L, m, d, T)$, if the system is finite. If one looks at these results, displayed in Fig. 2, one sees that the exponential tail wanders toward $t = \infty$ with increasing N , but it is quite unclear where the decay proportional to t^{-3}

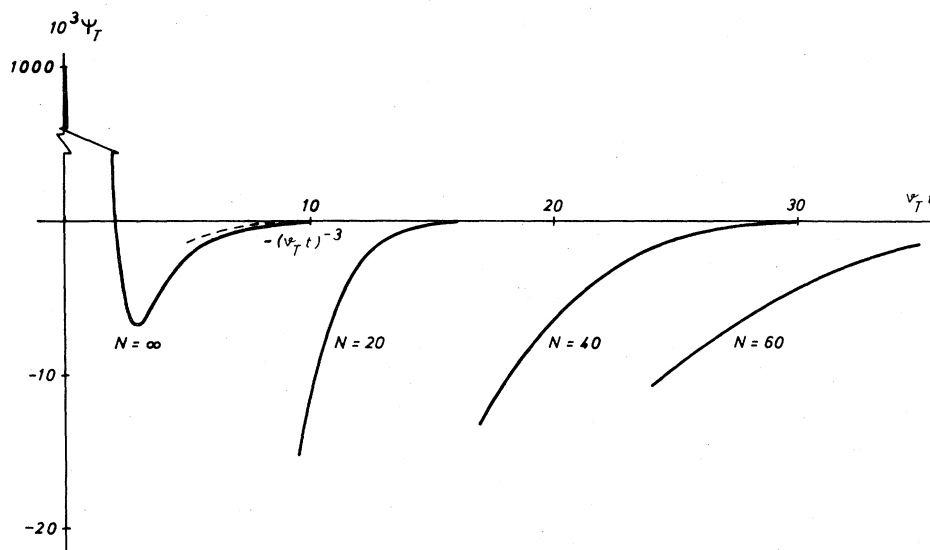


FIG. 2. Asymptotics of the velocity autocorrelation function ψ_T for $N=20,40,60,\infty$.

comes from.

To get a better insight into the nature of the TDL we calculated expectation values of phase-space functions for fixed parameters N, L, m, d first and passed then to the thermodynamic limit. This is the pattern in which Lebowitz and Sykes¹³—and, with some restrictions, also Jepsen¹⁵ and Evans¹⁴—obtained their results.

The first of the functions we investigated is the pair distribution function giving the number of particles which are expected to be found in a certain distance from a randomly chosen particle. Our results of this and more general spatial distribution functions are similar to those of Tonks¹¹ and Leff and Coopersmith,¹² the difference originating from the different definitions of the system (fixed walls versus movable box and fixed c.m.). It should be noted that the derivations are also different: Tonks assumed equal probabilities for all admissible configurations (without proving that this is a necessary condition for almost all stationary distribution functions), Leff and Coopersmith start from the partition function for the canonical ensemble, whereas we use the fact that every stationary ensemble may be viewed as a collection of smallest stationary ones. In the thermodynamic limit all functions converge to the pair distribution found by Zernike and Prins¹⁶ on heuristic grounds (see also Ref. 23) and rigorously derived by Salsburg *et al.*²⁵

The next quantity of interest is the pressure. Tonks¹¹, using the virial of Clausius and the Boltzmann equation, obtained the pressure for a canonical ensemble. The equation of state obtained this way corresponds to a van der Waals gas with purely repulsive forces ($a=0$). Frisch² defined a local pressure and discussed its evolution in time, but this pressure is not related to any collisions which are absent in his model. Carmona and Gottdiener²⁶ considered the motion of a mass point inside a dihedron and defined the pressure as time average of the momentum transferred to the walls. Their computer experiment turns out to be one way to calculate the pressure of the four-

particle system considered here. Ikeda and Takano²⁷ used the partition function of the canonical ensemble to obtain a true van der Waals equation ($a > 0$) but this result is obtained from a mere shift of the energy scale, not a different dynamics. Our method to calculate the pressure differs from these approaches already from the beginning. We define the pressure as the time average of the force acting onto a particle from its left. To this end we define a phase-space function measuring the increase of the particle's momentum caused by collisions with its left neighbor and average over a smallest stationary ensemble. For the microcanonical and the canonical ensembles the pressure is obtained by further averages and these results are compared with those derived from partition functions. For the microcanonical ensemble the results agree only in the thermodynamic limit, whereas for the canonical they coincide for all $N \geq 2$.

The calculation of the pressure is similar to that of the collision frequency which tells us how often, on the average, one of the particles hits its neighbors per unit time. This quantity defines a natural scale for time-dependent phenomena, especially in the thermodynamic limit, and is implicitly contained in the work of Jepsen¹⁵ and Lebowitz and Percus.¹⁷ A formal definition and explicit calculation has not been given in these papers but is provided in the following for the three ensembles mentioned above.

If ν is the collision frequency and δt an infinitesimal time interval then $\nu \delta t$ is the probability that a particle labeled with an arbitrary but fixed number undergoes a collision within the time interval $(0, \delta t)$. The corresponding probability for a finite interval is $\bar{W}(t)$ and $W(t) = 1 - \bar{W}(t)$ is the no-collision probability, i.e., the probability that a particle moves freely for a period of length t (or more). Like the collision frequency the form of $W(t)$ for $N = \infty$ and temperature T is implicitly contained in the results of Lebowitz and Percus.¹⁷ Our contribution consists in discussing the form of this function for the three ensembles and calculating it explicitly for

given energy and $2 \leq N \leq \infty$.

The quantity showing the strongest dependence on the size of the system is the velocity autocorrelation function (VAF). For the one-particle system corresponding to our two-particle system this function has been calculated by Nossal⁹ for the canonical ensemble and by Deutch *et al.*⁷ also for the microcanonical one. For the infinite system and the canonical ensemble Jepsen¹⁵ found the t^{-3} tail while Lebowitz and Percus¹⁷ computed the whole function. (These authors calculated it also for two other ensembles.) As regards systems with $2 < N < \infty$ Lebowitz and Sykes¹³ computed the VAF for rather special stationary ensembles corresponding to strictly periodic motions and performed the thermodynamic limit explicitly. Evans,¹⁴ following Jepsen,¹⁵ found a series representation for the VAF for given temperature and used it to extract the long-time behavior for finite systems. He also proved that this series converges to the function given by Lebowitz and Percus¹⁷ for $N \uparrow \infty$, but did not calculate explicitly any member of this sequence. We approach the problem from two sides: First we derive a power-series representation useful for short times ($0 \leq vt \leq 5$), then a sort of Fourier-series representing the VAF for all times. These series are evaluated numerically for $N \leq 40$, both for the microcanonical and the canonical ensemble. For the latter this series can be transformed into an integral which allows us to calculate the function for $N \leq 100$ and to pass finally to the thermodynamic limit where the VAF of Lebowitz and Percus¹⁷ is obtained once more.

We conclude this section with a few words on our method of calculation. Its basic idea is to replace a complicated motion in a bounded domain by a free motion in an infinite space endowed with a certain structure. The underlying "reflection trick," attributed to Lord Kelvin, has already been used by Born,⁶ Nossal,⁹ Hobson and Loomis,¹⁰ and Deutch *et al.*,⁷ for one particle within fixed walls. Once the trick has been applied to this system, corresponding to $N=2$ here, the advantage of using Fourier series is evident. A generalization of the method to $N=3$ has been discussed by Hobson²⁸ but not used for calculations of expectation values. To treat hard-rod systems with $2 < N < \infty$, a quite different-looking technique has been developed by Jepsen¹⁵ and used later on by Lebowitz and co-workers,^{17,13} Levitt,¹⁹ and Evans.¹⁴ Observing that in a collision velocities are conserved but "jump" from one particle to the other Jepsen followed the uniform motion of such a "velocity ray" through the volume. In a ring system the pulse returns after a while but in an infinite system no such pulse ever comes back which simplifies the dynamics.^{17,19} In this picture the reflection trick was only used to relate an N -particle system with fixed walls to a ring system with $2N$ particles.¹⁴ We use this trick extensively generalizing the methods of Born⁶ and Hobson²⁸ to arbitrary $N < \infty$. This yields a description of the system's evolution in geometrical terms which is very intuitive though it is slightly more difficult to recognize the motion of the individual particles in this approach than in Jepsen's scheme. Series representations introduced by Jepsen and his followers in a purely formal manner emerge here quite naturally, for the method makes obvious that the problems considered here are very

similar to problems in theoretical solid-state physics and can therefore be handled in quite a similar way.

III. TWO PARTICLES

If $x_{1,2}$ are the positions of the centers of the two particles a configuration is given by the vector $X=(x_1, x_2)$. To display the situation graphically it is more convenient to use $\bar{X}=(\bar{x}_1, \bar{x}_2)$ with

$$\bar{x}_1 = (1/\sqrt{2})(-x_1 + x_2), \quad \bar{x}_2 = (1/\sqrt{2})(x_1 + x_2), \quad (5)$$

instead of X . X and \bar{X} are uniquely related to each other by an orthogonal transformation, $\bar{X} = \mathcal{W}X$. To facilitate comparison with larger systems we write

$$X = X' + X'' \quad (6)$$

where

$$\mathcal{W}X' = \bar{X}' = (\bar{x}_1, 0), \quad \mathcal{W}X'' = \bar{X}'' = (0, \bar{x}_2). \quad (7)$$

If the same conventions are used for velocities, then (1) reads

$$X'' = 0, \quad V'' = 0, \quad (8)$$

and the "internal state" of the system is given by

$$Z' = (X', V'). \quad (9)$$

The confinement by the movable box is expressed by $|x_1 - x_2| < L - d$ and the fact, that the particles cannot penetrate through each other, by $|x_1 - x_2| > d$. The configuration space is therefore $S_1 \cup S_2$,

$$S_1 = \{X' \mid x_2 - L + d < x_1 < x_2 - d\}, \quad (10)$$

$$S_2 = \{X' \mid x_1 - L + d < x_2 < x_1 - d\},$$

and the phase space decomposes into two strips, i.e., $Z' \in (S_1 \times \mathbb{R}) \cup (S_2 \times \mathbb{R})$. A typical evolution of an initial state Z'_0 in phase space is illustrated in Fig. 3. If $S[X'_0]$ is the interval containing X'_0 ,

$$S[X'_0] = S_r \quad \text{if and only if } X'_0 \in S_r, \quad (11)$$

then $Z'_t \in S[X'_0] \times \mathbb{R}$ for all t (conservation of order).

Let us now explain the reflection trick for $d=0$. Start-

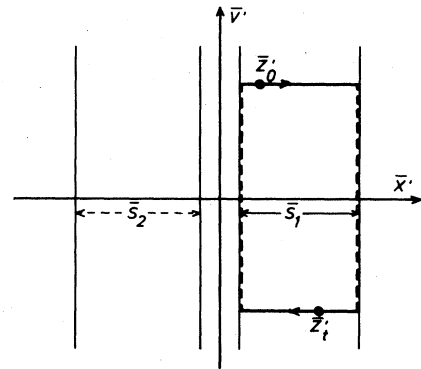


FIG. 3. Evolution in phase space ($N=2$).

these equations have to be completed by

$$f_0^s(X, V) = f_0(X, V) \chi^s(X'), \quad (24)$$

$$f_t^s(X, V) = \sum_s f_t^s(X, V). \quad (25)$$

The evolution of a general initial distribution f_0 is of interest for discussing time-dependent phenomena such as the approach to equilibrium.

To calculate expectation values for stationary ensembles it is sufficient to consider the (nonstationary) distributions

$$f_{V_0}^s(X, V) = (\sqrt{2}/L) \chi^s(X') \delta(V' - V_0') \delta(X'') \delta(V'') \quad (26)$$

since (almost) all stationary distributions can be expressed as superpositions of distributions of this form. Equation (26) means that the initial velocities are completely fixed but all configurations with a given order s are equally probable. The corresponding states Z_0' are then distributed along the interval $X' \in S_s$, $V' = V_0'$, and their evolution is uniquely determined by the free motion of this interval through the extended phase space R^2 . The probability that, starting with the distribution (26), the velocities are (still or again) the initial ones ($V_t' = V_0'$) is then the length of the intersection of

$$S[X_0'] + V_0't = \{X' + V_0't \mid X' \in S[X_0']\} \quad (27)$$

with the A segments divided by $L/\sqrt{2}$, while the intersection with the B segments is $L/\sqrt{2}$ times the probability that $V_t' = -V_0'$.

For $d > 0$ the general scheme is the same but some details have to be modified. First of all the volume L has to be replaced by the effective volume

$$L_d = L - 2d \quad (28)$$

in (12). The periodic structure is now generated by $S_1 + D_1$ or $S_2 + D_2$ ($= \mathcal{P}_2[S_1 + D_1]$),

$$D_1 = (d/2, -d/2) = -D_2, \quad (29)$$

and the cell of the lattice is

$$C = \bigcup_{\mathcal{P}} \mathcal{P}[S_1 + D_1]. \quad (30)$$

Therefore Eqs. (18) and (23) have to be replaced by

$$\bar{f}_0^s(X, V) = \sum_{\mathcal{P}, B} f_0^s(\mathcal{P}^{-1}[X - D_s - B], \mathcal{P}^{-1}V), \quad (31)$$

$$f_t^s(X, V) = \bar{f}_t^s(X + D_s, V) \chi^s(X'). \quad (32)$$

Turning now to the discussion of ergodic properties one sees immediately from Fig. 3 that the system is not ergodic with respect to the whole energy surface but only to half of it (or even less if $V_0' = 0$). That is, for almost all initial states Z_0'

$$\lim_{\tau \rightarrow \infty} \left[\frac{1}{\tau} \int_0^\tau dt g(X_t, V_t) \right] = |S|^{-1} \int_{S[X_0']} dX \left[\frac{1}{N!} \sum_{\mathcal{P}} g(X, \mathcal{P}V_0) \right]_{X''=0} \quad (33)$$

with $|S| = L_d/\sqrt{2}$ and $N=2$. Those Z_0' for which (33) does not hold are of the form $(X_0', 0)$; since they form a set of measure zero they are excluded from the following discussion. The ensemble over which the average is performed on the right-hand side (rhs) of (33) is one of the smallest stationary ones; that it coincides with a microcanonical one, constrained to a given order, will prove to be a special feature not present for $N > 2$. Another consequence of this exceptional behavior is the fact that for $N=2$ the evolution is strictly periodic no matter what the initial state Z_0' has been.

The approach to equilibrium of this system is, on the other hand, quite typical. Loosely speaking a certain spread of the velocities, compatible with

$$\sum_{i=1}^N v_i = 0,$$

is demanded in the beginning for a sort of irreversible behavior to occur. Let the function F_0 be defined by

$$F_0(V') = \int dX dV'' f_0(X, V); \quad (34)$$

then a sufficient condition for the existence of a weak limit $f_t \rightarrow f_{(\infty)}$ is the following hypothesis:

$$F_0 \text{ is a continuous function.} \quad (35)$$

Since F_0 is continuous it may be approximated by a superposition of characteristic functions of small intervals. Denoting such an interval by $\Delta V_0'$, its content by $|\Delta V_0'|$, and its characteristic function by $\chi^{\Delta V_0'}$, it is therefore sufficient to consider initial distributions of the form

$$f_0(X, V) = \delta(X' - X_0') |\Delta V_0'|^{-1} \chi^{\Delta V_0'}(V') \delta(X'') \delta(V''). \quad (36)$$

The evolution of this function and its extension \bar{f} is illustrated in Fig. 5. As time proceeds the initial segments obtained from $\{X_0'\} \times \Delta V_0'$ by periodic continuation wander and stretch out since points belonging to higher velocities move faster. This gives rise to a uniform hatching of the rectangles $S[X_0'] \times (\pm \Delta V_0')$ yielding the same expectation values as the normalized characteristic function of this area. It is easily recognized from Fig. 5 that the randomization of the positions is due to the finite volume only² while that of the velocities is caused by the collisions. For a general f_0 satisfying the hypothesis (35) the equilibrium distribution $f_{(\infty)}$ is given by

$$f_{(\infty)}(X, V) = \sum_s c_s \chi^s(X') \left[\frac{1}{N!} \sum_{\mathcal{P}} F_0(\mathcal{P}V') \delta(X'') \delta(V'') \right], \quad (37)$$

$$c_s = \int dX dV f_0(X, V) \chi^s(X'), \quad (38)$$

with $N=2$ and F_0 given by (34). How fast the equilibrium expectation values are obtained depends on the form of the initial distribution f_0 and the observable under consideration. Relaxation times for specific examples have been derived by Born,⁶ Teramoto and Suzuki,⁸ and Hobson and Loomis.¹⁰

Because of the simplicity of the system most of the ex-

pectation values can be written down immediately. The expectation value of $\delta(x_i - x_j - r)$ is the same for all stationary ensembles belonging to a given order because this quantity does not depend on the velocities. The pair distribution function, yielding the probability for finding the particles at a distance r , is

$$g(r) = \frac{1}{2} (\langle \delta(x_1 - x_2 - r) \rangle + \langle \delta(x_2 - x_1 - r) \rangle) \\ = \begin{cases} 0 & \text{for } |r| < d \text{ and } |r| > L - d \\ 1/2L_d & \text{otherwise.} \end{cases} \quad (39)$$

That g is constant where it is different from zero is atypical for the finite systems considered here.

The pressure p is defined as time average of the momentum transferred to one of the particles from its left neighbor. (If $x_1 < x_2$ particle 2 is the left neighbor of particle 1 because of the box.) Starting with $x_{10} < x_{20}$ and considering particle 2 we therefore have to count those collisions for which $v_1 > v_2$ before the collision. The number of these collisions comes arbitrarily close to $\tau(v_{10} - v_{20})/L_d$ if the interval $(0, \tau)$ is sufficiently large (see Figs. 3 and 4). The momentum transferred in each of these collisions is $m(v_{10} - v_{20})$. The time average and hence the average over the smallest stationary ensemble characterized by the order $x_1 < x_2$ and the set of initial velocities $\{v_{i0}\}$ is therefore

$$p_{\{v_{i0}\}} = (m/2L_d)(v_{10} - v_{20})^2. \quad (40)$$

Using (1) this may be rewritten in terms of the total energy

$$E = (m/2)(v_{10}^2 + v_{20}^2), \quad (41)$$

$$p_E = 2E/L_d.$$

To obtain the result for the canonical ensemble [with order and constraint (1)] one has to integrate (41) weighting the energy by

$$h_T(E) = (k_B T / \pi E)^{1/2} \exp(-E/k_B T). \quad (42)$$

This leads to the equation of state,

$$p_T = k_B T / L_d. \quad (43)$$

The collision frequency ν is defined as the average number of collisions of one of the particles per unit time. In the present case this average equals the number of all collisions per unit time. With similar reasoning as in the derivation of the pressure one finds

$$\nu_{\{v_{i0}\}} = (1/L_d) |v_{10} - v_{20}|, \quad (44)$$

$$\nu_E = (2/L_d) \sqrt{E/m}, \quad (45)$$

$$\nu_T = (2/L_d) \sqrt{k_B T / m \pi}. \quad (46)$$

The no-collision probability $W(t)$ is the probability that a tagged particle moves freely during the time interval $(0, t)$. It follows from this definition that $W(t)$ is monotonically decaying. From what has been said at the beginning of this section and inspection of Fig. 4 this probability is for a nonstationary distribution of the form (26)

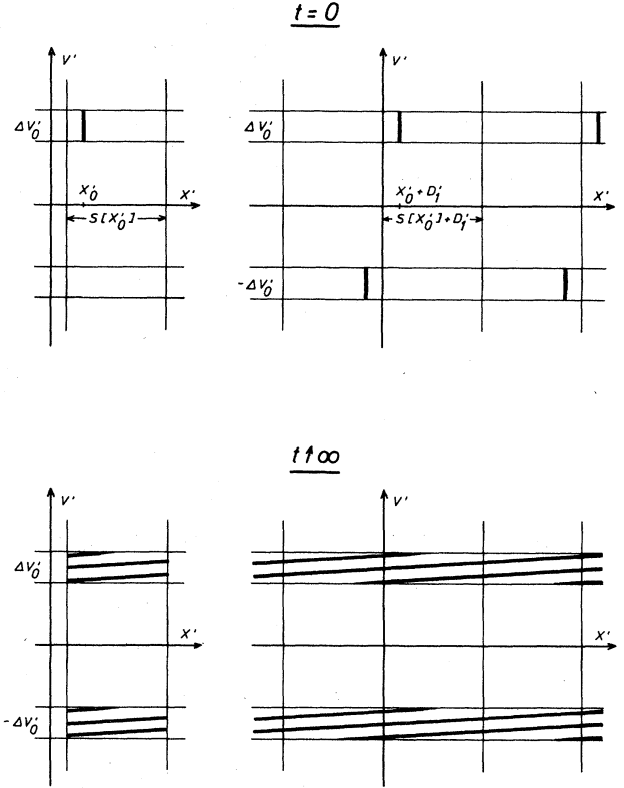


FIG. 5. Approach to equilibrium ($N=2$).

given by

$$W_{V'_0}(t) = |S|^{-1} |S_s \cap (S_s + V'_0 t)| \quad (47)$$

where $|\dots|$ denotes the length of the interval. This function is linearly decreasing from 1 to 0 remaining zero for all $t \geq L_d / |v_{10} - v_{20}|$. Averaging over $\pm V'_0$ does not change this function; hence

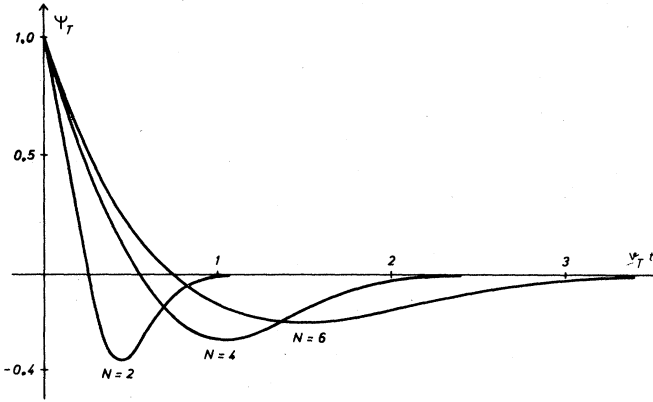
$$W_{\{v_{i0}\}}(t) = \begin{cases} 1 - \nu_{\{v_{i0}\}} t & \text{for } 0 \leq \nu_{\{v_{i0}\}} t \leq 1 \\ 0 & \text{for } 1 \leq \nu_{\{v_{i0}\}} t < \infty. \end{cases} \quad (48)$$

The division of the domain into intervals and the representation of the function by polynomials, one for each interval, is typical for $W_{\{v_{i0}\}}$ (or W_E obtained from $W_{\{v_{i0}\}}$ by substituting $\{v_{i0}\} \rightarrow E$). Atypical is only the fact that here the whole domain $(0, \infty)$ splits into two intervals only so that W_T may be obtained from W_E by integration.

The velocity autocorrelation function (VAF) is the expectation value of $v_{i0}v_{it}$. Setting $i=1$ and observing that $v_2 = -v_1$ for all times one finds $v_{10}v_{1t} = v_{10}^2$ for all $X'_t \in S[X'_0] + B$ (label A in Fig. 4) and $v_{10}v_{1t} = -v_{10}^2$ for $X'_t \notin S[X'_0] + B$ (label B in Fig. 4). For a distribution of the form (26) or the superposition $(f_{V'_0} + f_{-V'_0})/2 = f_{\{v_{i0}\}}$ representing a smallest stationary ensemble the normalized VAF

$$\psi(t) = \langle v_{i0}v_{it} \rangle / \langle v_{i0}^2 \rangle \quad (49)$$

is therefore given by the sawtooth curve⁷

FIG. 6. Velocity autocorrelation function ψ_T for $N=2,4,6$.

$$\psi_{\{v_{i0}\}}(t) = \begin{cases} 1 - 2\nu_{\{v_{i0}\}}t & \text{for } 2n \leq \nu_{\{v_{i0}\}}t \leq 2n+1 \\ -1 + 2\nu_{\{v_{i0}\}}t & \text{for } 2n+1 \leq \nu_{\{v_{i0}\}}t \leq 2n+2 \end{cases} \quad (50)$$

This function is also the VAF for the microcanonical ensemble. Equation (50) shows that $\psi_E(t)$ starts at $1 - 2\nu_E t$, a property which persists for larger systems up to the thermodynamic limit. A similar asymptotic form, namely $1 - 4\nu_T t + O(t^2)$, is found for ψ_T . What distinguishes $\psi_{\{v_{i0}\}}$ (or ψ_E) from ψ_T even more than the different slopes at $t=0$ is the fact that the first function may be defined by a sequence of polynomials, each representing it within one of an infinite number of intervals the union of which forms the whole domain. The strict periodicity of $\psi_{\{v_{i0}\}}$ will turn out to be atypical but it allows one to represent $\psi_{\{v_{i0}\}}$ as Fourier series. Substituting $\{v_{i0}\} \rightarrow E$ this series is⁷

$$\psi_E(t) = 8\pi^{-2} \sum_{n=0}^{\infty} (2n+1)^{-2} \cos[(2n+1)\pi\nu_E t]. \quad (51)$$

Its product with the weight function (42) can be integrated to yield^{9,7}

$$\psi_T(t) = 8\pi^{-2} \sum_{n=0}^{\infty} \exp\left[-\frac{1}{4}\pi^3(2n+1)^2\nu_T^2 t^2\right] \times \left[(2n+1)^{-2} - \frac{1}{2}\pi^3\nu_T^2 t^2\right]. \quad (52)$$

This function, displayed in Fig. 6, changes sign only once and has a tail proportional to $t^2 \exp(-\alpha t^2)$; these are general features, the first one persisting even to the thermodynamic limit.

We conclude this section by noting that all expectation values have been calculated for a fixed order, e.g., $x_1 < x_2$. Since all the results do not explicitly depend on this order they remain unchanged if one averages over both possible orders.

IV. THREE PARTICLES

We found it most useful to study the three-particle system in detail since this system exhibits all the typical

features of small systems ($N \leq 10$) and nearly all of arbitrary finite systems. Moreover, the small number of particles allows us to illustrate almost every calculation graphically which helped us to develop strategies for larger systems. A configuration of the three-particle system is given by $X = (x_1, x_2, x_3)$ or $\bar{X} = (\bar{x}_1, \bar{x}_2, \bar{x}_3) = \mathcal{W}X$, the orthogonal transformation \mathcal{W} transforming x_3 into $(1/\sqrt{3})(x_1 + x_2 + x_3)$. For instance,

$$\begin{aligned} \bar{x}_1 &= (1/\sqrt{2})(x_1 - x_2), \\ \bar{x}_2 &= (1/\sqrt{6})(x_1 - 2x_2 + x_3), \\ \bar{x}_3 &= (1/\sqrt{3})(x_1 + x_2 + x_3). \end{aligned} \quad (53)$$

Setting $\bar{X}' = (\bar{x}_1, \bar{x}_2, 0)$, $\bar{X}'' = (0, 0, \bar{x}_3)$, we arrive again at Eqs. (6), (8), and "internal states" $Z' = (X', V')$. If the particles are ordered according to $x_1 < x_2 < x_3$ then the configuration X' belongs to

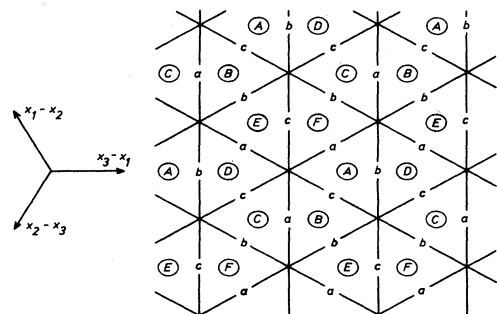
$$S_1 = \{X' \mid x_3 - L + d < x_1 < x_2 - d < x_3 - 2d\}. \quad (54)$$

Five more domains S_2, \dots, S_6 corresponding to the other possible orders are defined in a similar way. The regions S_s are all equilateral triangles of height $L_d/\sqrt{2}$,

$$L_d = L - 3d. \quad (55)$$

If $X'_0 \in S_s$ then $X'_t \in S_s$ for all t and if two particles collide the representative point X'_t is elastically reflected at one of the sides of the triangle. It is again possible to apply the reflection trick to obtain a simple covering of the plane \mathbf{R}^2 by equilateral triangles generated from S_s by iterative reflections along the sides of the triangles.²⁸

To simplify the calculation it is advantageous to shift $S_s = S[X'_0]$, and thereby the whole structure generated by this triangle, by a constant vector D depending on X'_0 and d ; for $d=0$ one has always $D=0$. The complicated motion of x'_i inside S_s may then be replaced by the uniform motion $X'_0 + D + V'_0 t$ but the "parquet" structure of triangles has to be labeled to recover from $X'_0 + D + V'_0 t$ not only the true position X'_t but also the true velocity V'_t . Figure 7 is an example of such a labeling showing both the distribution of the initial velocities v_{10}, v_{20}, v_{30} onto the particles 1, 2, 3, and which pair of particles is involved in a collision changing this distribution [e.g., $c:23$ for $A:(u, v, w) \rightarrow B:(u, w, v)$]. As in the case $N=2$ the



A: (u, v, w) D: (w, v, u) a: 12
 B: (u, w, v) E: (v, w, u) b: 13
 C: (w, u, v) F: (v, u, w) c: 23

FIG. 7. Extended configuration space ($N=3$).

meaning of the labels depends of course on the initial configuration X'_0 .

Let us now describe this structure in more detail. It is sufficient to consider it for $d=0$ ($D=0$) since all the following results except the pair distribution function are obtained for $d>0$ simply by substitution, viz., L_d for L . For $d=0$ the lines defining the structure are given by $x_i - x_j = n_{ij}L$, n_{ij} integer. The periodicity of the structure is described by a two-dimensional hexagonal lattice $\{B\}$, the symmetry-adapted cell of which is a regular hexagon. The six triangles forming the cell containing $X'=0$ are transformed into each other by six transformations \mathcal{P}_r generated by reflections along the lines $x_i = x_j$. Each transformation \mathcal{P} is an orthogonal transformation in \mathbb{R}^3 , uniquely related to a permutation $P:i \rightarrow Pi$ by

$$\mathcal{P}^{-1}(x_1, x_2, x_3) = (x_{P1}, x_{P2}, x_{P3}). \quad (56)$$

The lattice $\{B\}$ and the transformations \mathcal{P} may be used to solve the Liouville equation in a similar way as for $N=2$. In fact, if the vectors and transformations appropriate for $N=3$ are used, Eqs. (17) to (25) relating f_0 to f_t are valid also here. For $N=3$ the singularities of the function \tilde{f}_0^s , Eq. (19), form six ($=3!$) lattices transforming into each other under the transformations \mathcal{P} . As time proceeds these lattices move uniformly with velocities $\mathcal{P}V'_0$. The triangle $S[X'_0]$ always contains one and only one point of these six lattices and its position and velocity are just X'_t and V'_t .

As in the case $N=2$ it may be sometimes more convenient to consider the ray $X'_0 + V'_0 t$, $t \geq 0$, or a collection of such rays, $X'_0 \in S_s$, instead of the corresponding distribution functions (17) or (26). The relation between the multiply reflected motion of X'_t in the true configuration space and the uniform motion $X'_0 + V'_0 t$ in the extended configuration space is shown in Fig. 8. The state $Z'_t = (X'_t, V'_t)$ is obtained from $X'_0 + V'_0 t$ again by Eqs. (14) where \mathcal{P} and B are uniquely determined by $\mathcal{P}(X'_0 + V'_0 t + B) \in S[X'_0]$. Note that the ray $X'_0 + V'_0 t$, $t \geq 0$, considered here corresponds now to three trajectories in Jepsen's scheme. Two of these trajectories cross each other whenever $x'_0 + V'_0 t$ hits a line $x_i - x_j = n_{ij}L$. If the ray passes a point where three such lines cross each other then all three particles collide. The ray (or the corresponding trajectories in Jepsen's diagram) then defines what happens in such a triple collision, i.e., how the velocities before and after the collision are related. This definition is a very natural one because an infinitesimal variation of initial conditions causing an infinitesimal difference in the final-state changes the triple collision into a sequence of binary collisions for which the dynamics has been already defined.

The ergodic properties of this system have been discussed by Hobson²⁸ in a more general context (motion of a particle inside a polygon). He recognized the existence of conserved quantities beside the total energy which in our interpretation of the system are just the order of the particles and the set of initial velocities. He conjectured (but did not prove) that the evolution is ergodic with respect to the "small" subset of the energy surface characterized by prescribed values of the conserved quantities (the order s , given by $x'_0 \in S_s$, and the set $\{v_{i0}\}$ in the present case).

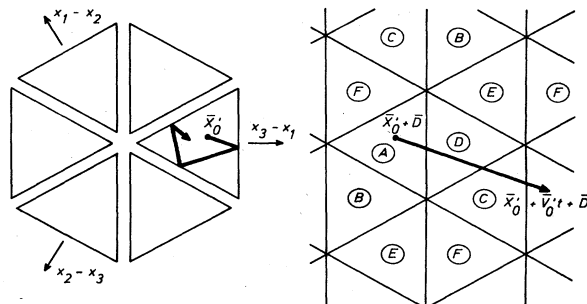


FIG. 8. Evolution in true and extended configuration space ($N=3$).

We will prove this elsewhere quite generally for the N -particle system and almost all initial states Z'_0 . The proof is similar to that of a theorem on uniform distributions due to Kronecker and Weyl^{29,30} and its basic idea is already evident from the following heuristic argument: Consider the line $X'_0 + V'_0 t$, $0 \leq t \leq \tau$, τ very large. All its points contribute to the time average of an observable g ; however, not directly but only through their meaning for X'_t and V'_t . Instead of bringing back all points to the true phase space $S[X'_0] \times \mathbb{R}^2$ according to (14) one can equally well extend the domain of $g = g^s$ by means of (18) and integrate the new function \tilde{g}^s , obtained from g^s by successive reflections, along the line $X'_0 + V'_0 t$, $0 \leq t \leq \tau$. Now chose a parallelepiped containing six triangles as cell of the lattice $\{B\}$, divide the extended configuration space \mathbb{R}^2 into cells of this shape, and shift the intersections of the line with the cells by suitable lattice vectors all back into the cell containing X'_0 . It is plausible to assume that this yields a uniform hatching of the cell by parallel lines which is denser the larger τ is (see Fig. 9). In fact Weyl's theorem tells us that this happens for almost all $V'_0 \in \mathbb{R}^2$, independently of X'_0 . Whether \tilde{g}^s is integrated along the line or along its segments shifted into one cell makes no difference; \tilde{g}^s is, by construction, a periodic function. If τ becomes large enough the parallel lines covering the cell become arbitrarily close so that for a smooth g the integral over the segments may be replaced by one over the whole cell. But the points of a cell are mapped onto the

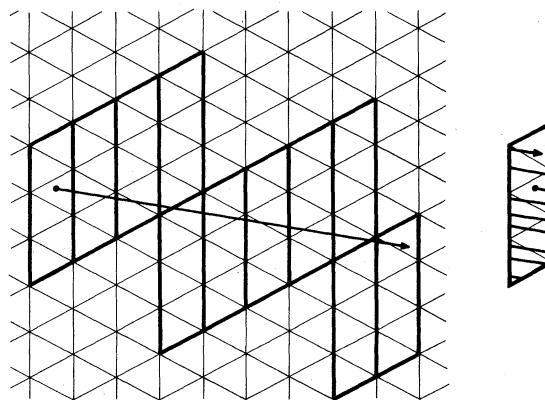


FIG. 9. Equivalence of time and ensemble average ($N=3$).

true phase space by (14) so that (33) is valid also for $N=3$.

The description of the evolution of the system by means of the ray $X'_0 + V'_0 t$ is also very suited for a discussion of recurrence times. If for some time $t > 0$ $V'_0 t$ is equal to a lattice vector B then it is clear from (14) that $Z'_t = Z'_0$ for this time, i.e., the system is in exactly the same state as at the beginning. This happens if and only if the ratios $w_{ij}:w_{kl}, w_{ij} = v_i - v_j$ are rational numbers. Initial states leading to strictly periodic motions are therefore dense in phase space but of measure zero. For a "typical" initial state the ratios $w_{ij}:w_{kl}$ are irrational; but since they may be approximated by rationals to any desired degree of accuracy there always exist times t where $V'_0 t$ is arbitrarily close to a lattice vector B . Every function $H(t) = h(X_t, V_t)$ is therefore almost periodic (even in the technical sense³¹) and this carries over to expectation values $\langle g(X, V)h(X_t, V_t) \rangle_{\{v_{i0}\}}$ since the "periods" are independent of X'_0 and the same for all velocities $\mathcal{P}V'_0$.

All these statements on recurrence times and the equivalence of time and ensemble averages should be familiar to readers acquainted with the foundations of modern (nonlinear) dynamics.^{32,33} In fact the (typical or general) smallest stationary ensembles introduced here are just the (irrational or nonresonant) invariant tori appearing there. That the hard-rod systems considered here are integrable will be shown in full detail elsewhere.

Regarding the approach to equilibrium it is straightforward to generalize the arguments for $N=2$ to obtain a similar result for $2 < N < \infty$. In the present case the equilibrium distribution $f_{(\infty)}$, which is the weak limit of an initial distribution satisfying (35), is again given by Eqs. (37), (38), and (34), specialized to $N=3$.

Let us now consider expectation values. For (almost) all stationary distributions f

$$\int dX'' dV f(X, V) = c_s \quad \text{for } X' \in S_s, \quad (57)$$

i.e., the spatial distribution on the left-hand side (lhs) is constant within each of the six triangles forming the configuration space. For a (typical) smallest stationary ensemble $c_s = \delta_{sr}$, where $S_r = S[X'_0]$ if the average is interpreted as time average. To calculate $\langle \delta(x_i - x_j - r) \rangle_s$ one therefore has to determine the length of the interval obtained from intersecting the line $x_i - x_j = r$ with the triangle S_s and to divide it by the area of S_s . Note that the length of the interval depends on d since both the size and the position of the triangle S_s depend on this quantity [cf. Eq. (54) and the lhs of Fig. 8]. If the pair distribution function is defined by

$$g(r) = \frac{1}{3} \sum_{\substack{i,j=1 \\ i \neq j}} \langle \delta(x_i - x_j - r) \rangle_s, \quad (58)$$

the result is independent of s because of the summation occurring in (58). The function (58) is displayed in Fig. 10 for $d = (1/5)L$ and $d=0$, respectively. The linear decrease in the region $0 < |r| < L$ is typical for $d=0$. For $d > 0$ it is a typical feature that the function has maxima where it changes from zero to positive values, the main maximum being at $|r| = d + 0$.

To calculate the pressure we start again with its defini-

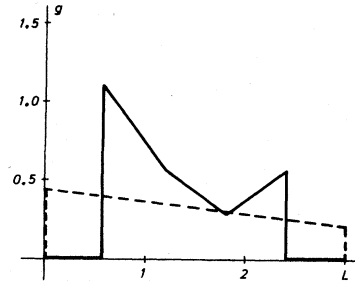


FIG. 10. Pair distribution function for $N=3$ (solid line $d=0.6/\rho$; dashed line $d=0$).

tion as time average and study the evolution by means of the ray $X'_0 + V'_0 t$, $t \geq 0$. If $d=0$ a collision occurs whenever the point of the ray hits one of the lines $x_i - x_j = n_{ij}L$ (see Fig. 8). If a line $x_1 - x_2 = n_{12}L$ is crossed this corresponds to a collision where $v_{i,t-0} = v_{j,t+0} = v_1$, $v_{j,t-0} = v_{i,t+0} = v_2$ for some pair i, j . For large τ the number of these collisions within the period $(0, \tau)$ is arbitrarily close to $\tau |v_{10} - v_{20}| / L$. Only one-third of it may be attributed to a given pair. If, for instance, the pair 12 is considered then only those crossings of the ray with the lines $x_1 - x_2 = \text{const}$ have to be counted which are labeled by "a" in Fig. 7. Now if $v_{10} < v_{20}$ a crossing of a is a transition of type $F \rightarrow A$, i.e., $v_{1,t-0} = v_{20}$, $v_{2,t-0} = v_{10}$, and the increase of the momentum of particle 2 is equal to

$$m(v_{2,t+0} - v_{2,t-0}) = m(v_{20} - v_{10}) > 0.$$

Combining these results one obtains for the time average of the expectation value for the corresponding smallest stationary ensemble

$$p_{\{v_{i0}\}} = (m/3L)[(v_{20} - v_{10})^2 + (v_{30} - v_{20})^2 + (v_{30} - v_{10})^2]. \quad (59)$$

To obtain the expectation value for the microcanonical ensemble one has to take into account that the bracket in (59) is just $3(\bar{v}_{10}^2 + \bar{v}_{20}^2) = 3(V')^2$, and that the total energy is $E = mV'^2/2$. The rhs of Eq. (59) may therefore be transcribed as $2E/L$, and averaging over all directions of V'_0 with

$$|V'_0| = \sqrt{2E/m} \quad (60)$$

hold fixed, necessary to pass from the smallest stationary to the microcanonical ensemble, does not change this value. Therefore Eq. (41) (with $d=0$) is also valid for $N=3$. This expression has to be multiplied with the weight function

$$h_T(E) = (1/k_B T) \exp(-E/k_B T) \quad (61)$$

and integrated over E to obtain the pressure for the canonical ensemble

$$p_T = 2k_B T / L. \quad (62)$$

As in the case $N=2$ the calculation of the collision frequency is similar to that of the pressure. If one considers, for instance, the collisions of particle 2 in the time interval $(0, \tau)$ then all crossings of the ray with segments labeled by "a" or "c" have to be counted. Noting that these

segments cover two-thirds of every line one may similarly argue as one did before for the pressure to obtain

$$v_{\{v_{i0}\}} = (2/3L)(|v_{20}-v_{10}| + |v_{30}-v_{20}| + |v_{30}-v_{10}|). \quad (63)$$

To average over all directions of V'_0 with $|V'_0|$ fixed by (60) the relative velocities $v_{i0}-v_{j0}$ are expressed in terms of the variables \bar{v}_k . Introducing polar coordinates and carrying out the integration one finds

$$v_E = (8/L\pi)\sqrt{E/m}, \quad (64)$$

from which after one more integration

$$v_T = (4/L)\sqrt{k_B T/m} \quad (65)$$

is obtained.

The calculation of the no-collision probability $W(t)$ is illustrated in Fig. 11. The hatched area is the intersection of two triangles of the parquet structure with a shifted triangle. The two triangles, labeled by A and B in Fig. 7, correspond to velocity distributions where the velocity of the first particle is (still) v_{10} . The shifted triangle is $S[X'_0] + V'_0 t$, the union of all points $X'_0 + V'_0 t, X'_0$

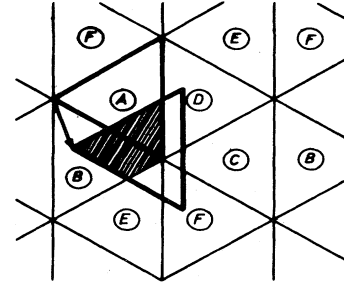


FIG. 11. Illustration of the calculation of the no-collision probability ($N=3$).

$\in S[X'_0]$ (label A), and the location of these points relative to the parquet structure shows in what states the system is expected to be found at time t . Thus if the area of the triangle is normalized to 1, the hatched area gives just the probability $W_{V'_0}(t)$ that particle 1 has not changed its velocity in the interval $(0, t)$. This result for a distribution function of the form (26) has to be averaged over the six velocities $\mathcal{P}V'_0$ to obtain the no-collision probability for a smallest stationary ensemble

$$\begin{aligned} W_{\{v_{i0}\}}(t) &= (1/3L^2)[(L - |v_{20}-v_{10}|t)_+ (L - |v_{30}-v_{10}|t)_+ + (L - |v_{10}-v_{20}|t)_+ (L - |v_{30}-v_{20}|t)_+ \\ &\quad + (L - |v_{10}-v_{30}|t)_+ (L - |v_{20}-v_{30}|t)_+] \\ &= 1 - v_{\{v_{i0}\}}t + O(t^2). \end{aligned} \quad (66)$$

The quantities $(\dots)_+$ appearing in (66) are defined by

$$a_+ = \frac{1}{2}(a + |a|) = \begin{cases} a & \text{for } a \geq 0 \\ 0 & \text{for } a < 0. \end{cases} \quad (67)$$

In (66) $W_{\{v_{i0}\}}$ is given as a polynomial of second degree in t but the form of this polynomial depends on which quantities $(\dots)_+$ vanish. That is, the domain of $W_{\{v_{i0}\}}$ splits into a finite number of intervals, all of finite length except the last one, and $W_{\{v_{i0}\}}$ is represented by a polynomial within each interval. We are especially interested in the first interval $(0, \tau)$,

$$\tau = \min_{i,j} \{t_{ij}\}, \quad t_{ij} = L/|v_{i0}-v_{j0}|, \quad (68)$$

and the corresponding "first polynomial" obtained from (66) by omitting the index $+$ everywhere. The function W_E has a similar structure. To obtain the first polynomial for this function we note that

$$|v_i - v_j| \leq \sqrt{2} |V'|. \quad (69)$$

Hence if

$$t < L/\sqrt{2} |V'_0| \quad (70)$$

$W_{\{v_{i0}\}}$ is given by its first polynomial and this holds independently of the direction of V'_0 . Averaging over the directions of all these vectors with length (60) can therefore be performed for each term separately. The result is

$$W_E(t) = 1 - v_E t + \frac{1}{32} \pi (\sqrt{3} + \frac{1}{6} \pi) v_E^2 t^2 \quad \text{for } 0 \leq v_E t M = 4/\pi. \quad (71)$$

For $v_E t > 4/\pi$, W_E decreases monotonically reaching its final value zero at $v_E t = 8/\pi$. Since the intervals where W_E is represented by a certain polynomial depend on E the function W_T is not simply obtained by averaging the coefficients of the first polynomial with the weight function (61). That only upper and lower bounds can be derived this way is typical for all finite systems.

To calculate the VAF for the three-particle system we start in a similar way as for the probability $W(t)$. If we consider a distribution function of the form (26) then $\langle v_{10} v_{1t} \rangle_{V'_0} = v_{10} \langle v_{1t} \rangle_{V'_0}$, i.e., the calculation of the VAF reduces to that of v_{1t} . Proceeding as for $W_{V'_0}(t)$ we see from Fig. 12 that the task is again to calculate areas which are the intersections of parallelograms (where v_1 has one of the values v_{10}, v_{20}, v_{30}) with a shifted triangle [indicating the present state of all systems which started with $(X'_0, V'_0), X'_0 \in S_s$]. It is clear from Fig. 12 that the VAF is given by an infinite number of polynomials, each representing the function ψ in a certain time interval. These intervals arise if \mathbb{R} , the domain of ψ , is divided into segments by all integer multiples of the times t_{ij} defined in (68). If the first polynomial is calculated by inspection of Fig. 12 and the average over the six velocities $\mathcal{P}V'_0$ is performed one finds

$$\psi_{\{v_{i0}\}}(t) = (v_{10}^2 + v_{20}^2 + v_{30}^2)^{-1} \{ [v_{10}^2 + v_{20}^2 + v_{30}^2] - (t/L) (|v_{30} - v_{10}|^3 + |v_{30} - v_{20}|^3 + |v_{20} - v_{10}|^3) \\ + (t^2/2L^2) [(v_{10} - v_{20})^2 (v_{10} - v_{30})^2 - 6(v_{20} - v_{10})_+^2 (v_{10} - v_{30})_+^2 + \text{C.P.}] \}$$

for $t \leq \tau$, τ defined in Eq. (68), (72)

where C.P. stands for cyclic permutations of the preceding terms. Equation (72) can be used to determine $\psi_E(t)$ for short times. Expressing $|V'_0|$ by E according to (60) and averaging over all directions of V'_0 one obtains as first polynomial

$$\psi_E(t) = 1 - 2v_E t + (27\pi\sqrt{3}/256)v_E^2 t^2 \\ \text{for } 0 \leq v_E t \leq 4/\pi. \quad (73)$$

The same reasons that prevented W_T from being obtained by integrating W_E term by term prevent ψ_T being obtained from ψ_E this way. Again the integration of terms of (73) can only be used to obtain bounds for ψ_T or asymptotic formulas such as

$$\psi_T(t) = 1 - 3v_T t + O(t^2). \quad (74)$$

The first polynomial is only useful to discuss the short-time behavior of ψ . One knows from general considerations that $\psi_{\{v_{i0}\}}$ is an almost periodic function and expects ψ_E and ψ_T to decay for $t \uparrow \infty$. To verify this long-time behavior one has to find representations of these functions valid for large times. Actually series representations valid for all times can be found; why this is possible and of what form these series are is nicely displayed on the present example. The first step is to express the area of the intersection of two domains as integral over the product of their characteristic functions. In the present case one of the domains is the shifted triangle $S_s + V'_0 t$ with characteristic function $\chi^s(X' - V'_0 t)$. The other domain is composed of triangles of the form $S_r + B$ with characteristic functions $\chi^r(X' - B)$. We may replace $S_r + B$ by

$$\bigcup_B (S_r + B)$$

since only one of these triangles has a nonempty intersection with $S_s + V'_0 t$. Denoting the area of a set M by $|M|$ we therefore have

$$\left| (S_s + V'_0 t) \cap \left[\bigcup_B (S_r + B) \right] \right| \\ = \int dX' \chi^s(X' - V'_0 t) \sum_B \chi^r(X' - B). \quad (75)$$

The second function in the integral is obviously periodic in X' ; it is therefore natural to express it as a generalized Fourier series. To this end one needs the lattice $\{A\}$ which is reciprocal to $\{B\}$. This lattice is also a two-dimensional hexagonal lattice and it may be scaled in such a way that $\{B\} \subset \{A\}$. In this case one has, for all A, B ,

$$AB = \text{integer multiple of } 2\pi/\alpha, \quad \alpha = 2\pi/L^2, \quad (76)$$

and

$$\sum_B \chi^r(X' - B) = \sum_A \tilde{\chi}^r(A) \exp(i\alpha A \cdot X'), \quad (77)$$

$$\tilde{\chi}^r(A) = |C|^{-1} \int_C dX' \chi^r(X') \exp(-i\alpha A \cdot X') \\ = |C|^{-1} \int_{S_r} dX' \exp(-i\alpha A \cdot X'), \quad (78)$$

where C is a cell of $\{B\}$, e.g., the hexagon

$$\bigcup_s S_s.$$

Introducing (77) into (75) yields integrals which can be expressed by means of coefficients of the form (78)

$$\int dX' \chi^s(X' - V'_0 t) \exp(i\alpha A \cdot X') \\ = \int dX' \chi^s(X') \exp[i\alpha A \cdot (X' + V'_0 t)] \\ = \exp(i\alpha A \cdot V'_0 t) \tilde{\chi}^{s*}(A). \quad (79)$$

Denoting the velocity distribution belonging to S_r by $(v_1)_r, (v_2)_r, (v_3)_r$ one therefore has

$$\langle v_{10} v_{1t} \rangle_{V'_0} = |S|^{-1} \sum_{r,A} v_{10} (v_1)_r \tilde{\chi}^{s*}(A) \tilde{\chi}^r(A) \\ \times \exp(i\alpha A \cdot V'_0 t). \quad (80)$$

Symmetrization with respect to the components of V'_0 gives

$$\langle v_{10} v_{1t} \rangle_{\{v_{i0}\}} = \sum_{A (\neq 0)} \gamma(A) (V'_0 \cdot A)^2 \exp(i\alpha A \cdot V'_0 t) \\ = -\frac{L^4}{4\pi^2} \frac{\partial^2}{\partial t^2} \left[\sum_{A (\neq 0)} \gamma(A) \exp(i\alpha A \cdot V'_0 t) \right]; \quad (81)$$

here the coefficients $\gamma(A)$ are uniquely determined by the coefficients $\tilde{\chi}^s(A)$ which can be calculated explicitly. Equation (81) makes obvious that $\langle v_{10} v_{1t} \rangle_{\{v_{i0}\}}$ is almost periodic because all exponentials are close to one, the value for $t=0$, if $V'_0 t$ is close to a lattice vector B . The function (81) has to be averaged over all directions of V'_0 to obtain the VAF for the microcanonical ensemble. If this integration transforming exponentials into Bessel

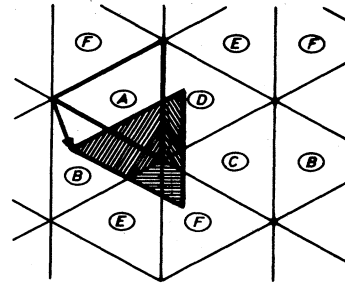


FIG. 12. Illustration of the calculation of the velocity auto-correlation function ($N=3$).

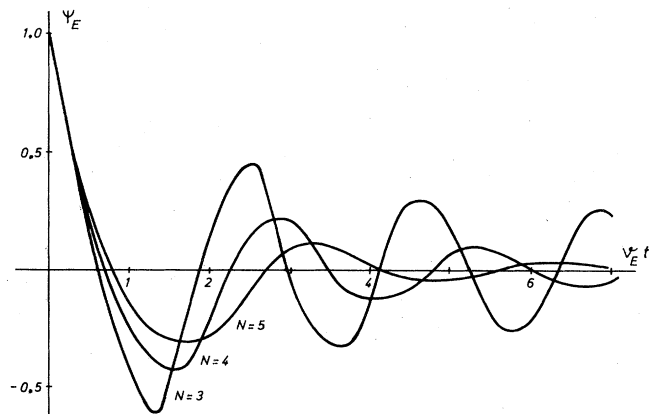


FIG. 13. Velocity autocorrelation ψ_E for $N=3,4,5$.

functions times powers is carried out, the lattice vectors A are parametrized by a pair of integers, and $\gamma(A)$ is expressed as a function of $\underline{n}=(n_1, n_2)$, one ends up with the function

$$\psi_E(t) = \sum_{\underline{n}}' c_{\underline{n}} [J_0(\sqrt{\pi s_{\underline{n}}} v_E t) - (\sqrt{\pi s_{\underline{n}}} v_E t)^{-1} J_1(\sqrt{\pi s_{\underline{n}}} v_E t)], \quad (82)$$

where

$$\sum_{\underline{n}}' = \sum_{n_1, n_2} \text{ with } n_1 \neq 2n_2, n_2 \neq 2n_1 \quad (83)$$

$$c_{\underline{n}} = \left[\frac{9 \sin^2[\frac{1}{3}(n_1 + n_2)\pi]}{\pi^2(2n_1 - n_2)(2n_2 - n_1)} \right]^2, \quad (84)$$

$$s_{\underline{n}} = [\frac{1}{12} \pi^3 (n_1^2 + n_2^2 + n_1 n_2)]^{1/2}. \quad (85)$$

The function (82), displayed in Fig. 13, oscillates infinitely often around zero with decreasing amplitude. This will be found for all finite systems but the power law of the decay, $t^{-1/2}$ in the present case, varies with the number of particles. Since (82) is valid for all times $\langle v_{10} v_{1t} \rangle_T = (2kT/3m)\psi_T(t)$ may be obtained from $\langle v_{10} v_{1t} \rangle_E = (2E/3m)\psi_E(t)$ by integration. The series

$$\psi_T(t) = \frac{1}{2} \sum_{\underline{n}}' c_{\underline{n}} (1 - 2s_{\underline{n}}^2 v_T^2 t^2) \exp(-s_{\underline{n}}^2 v_T^2 t^2) \quad (86)$$

has also been evaluated numerically; the resulting curve is quite similar to that for $N=2$ as shown in Fig. 6.

We conclude noting that for $d > 0$ L has to be substituted by L_d in all equations from (62) on. We also like to point out that all expectation values have been calculated for a given order of the particles. Since this order does not show up in the final results they remain unchanged if the average over all possible orders is performed.

V. MANY PARTICLES

The extensive treatment of the two- and three-particle systems should have prepared the ground for a discussion of the general N -particle system. We therefore focus on those results which, though straightforward generalizations of the previous ones, are not obvious or cannot be guessed at all.

That we are able to generalize the results for the cases $N=2$ and $N=3$ rests on the fact that the reflection trick

works also for $N > 3$. We can always pass from $X=(x_1, \dots, x_N)$ to $\mathcal{W}X=\bar{X}=(\bar{x}_1, \dots, \bar{x}_N)$ by means of an orthogonal transformation \mathcal{W} such that

$$\bar{x}_N = (1/\sqrt{N})(x_1 + x_2 + \dots + x_N), \quad (87)$$

with \bar{x}_N fixing the position of the center of mass, and $\mathcal{W}X''=\bar{X}''=(0, 0, \dots, 0, \bar{x}_N)$. For our model the internal configuration $\bar{X}'=(\bar{x}_1, \dots, \bar{x}_{N-1}, 0)$ is then confined to a simplex, the N th member of the sequence point ($N=1$), line ($N=2$), triangle ($N=3$), tetrahedron ($N=4$), etc. Guessing from the examples considered up to now the symmetries of these domains might be overestimated; actually the $(N-1)$ -dimensional simplex is not a regular one for $N > 3$. It has only a dihedral symmetry group, not one isomorphic to the full symmetric group. There are $N!$ such simplices transforming into each other under permutations of the coordinates of $X=(x_1, \dots, x_N)$. They stick together if $d=0$ but are separated by sheets of thickness $d/\sqrt{2}$ if $d > 0$ (see, e.g., Fig. 3 and the lhs of Fig. 7). This separation is only of interest for spatial properties (pair distribution function, etc.); for properties depending only on the evolution of the velocities (pressure, VAF, etc.) the scaling $L \rightarrow L_d$,

$$L_d = L - Nd, \quad (88)$$

is all that is needed. As time evolves the representative point X'_t moves inside of one of the simplices elastically reflected at its boundaries (cf. lhs of Fig. 8). But if the simplex $S[X'_0]$ is reflected on the boundary first hit by X'_t the first kink in the path X'_t , $0 \leq t \leq \tau$, is unfolded to a straight line. Repeating this procedure one ends up with a sequence of adjacent simplices connected by the ray $X'_0 + V'_0 t$, $0 \leq t \leq \tau$. It can be shown that the simplices generated from $S[X'_0]$ by iterative reflections along the boundaries form a simple covering of \mathbb{R}^{N-1} . This structure has the periodicity of a lattice $\{B\}$ which is the one-dimensional lattice for $N=2$, the two-dimensional hexagonal lattice for $N=3$, the face-centered-cubic lattice for $N=4$, etc. For $d=0$ the structure of the extended configuration space \mathbb{R}^{N-1} is given by the planes $x_i - x_j = n_{ij}L$, n_{ij} integer, and the reflections on the planes $x_i = x_j$ generate orthogonal transformations \mathcal{P} which leave the structure invariant and form a group isomorphic to \mathcal{S}_N , the symmetric group of degree N . The structure is also invariant under orthogonal transformations leaving one of the simplices invariant and forming a group isomorphic to D_N , the dihedral group of order $2N$. All these transformations of X may be extended to canonical transformations commuting with the evolution and exploited in the calculation of expectation values.

The discussion of ergodic properties of the N -particle system parallels completely that of the two- and three-particle system and the results are the same or straightforward generalizations of those obtained in Secs. III and IV. We therefore switch immediately to the expectation values calculated along the pattern described in the previous section. The weight function needed to pass from the microcanonical ensemble to the canonical one is now

$$h_T(E) = [(k_B T)^{(N-1)/2} \Gamma(\frac{1}{2}(N-1))]^{-1} E^{(N-3)/2} \times \exp(-E/k_B T). \quad (89)$$

If the pair distribution function is defined as

$$g(r) = (1/N) \sum_{\substack{i,j=1 \\ i \neq j}}^N \langle \delta(x_i - x_j - r) \rangle_s$$

$$= [(N-1)/N!] \sum_s \langle \delta(x_i - x_j - r) \rangle_s, \quad (90)$$

where s characterizes a stationary ensemble belonging to a given order, one has to calculate the content of the intersection of a plane $x_i - x_j = r$ with the simplices forming part of the (true) configuration space. By symmetry arguments this may be reduced to calculate the content of parallelepipeds. The result is

$$g(r) = \frac{(N-1)!}{NL_d} \sum_{n=0}^{N-2} \frac{(N-1-n)}{(N-2-n)!n!} \Theta(|r| - (n+1)d) \Theta(L_d - |r| + (n+1)d)$$

$$\times \left[\frac{|r| - (n+1)d}{L_d} \right]^n \left[1 - \frac{|r| - (n+1)d}{L_d} \right]^{N-2-n} \quad (91)$$

where $\Theta(x) = 1$ for $x > 0$ and $\Theta(x) = 0$ otherwise. The function $g(r)$ has been displayed in Fig. 14 for $N=5, 20$ and two ratios of d/L .

The pressure of the N -particle system may be obtained in three ways: The first is to guess the result from that for $N=2$ and $N=3$; the second is to repeat (and generalize) the heuristic arguments used in the previous sections; and the third is to calculate the desired expectation value quite formally with a phase-space function measuring the average momentum transfer. The first two approaches are left to the reader while the last one is part of the calculations to be presented elsewhere. The result is in any case

$$p_{\{v_{i0}\}} = (m/2NL_d) \sum_{i,j=1}^N (v_{i0} - v_{j0})^2, \quad (92)$$

$$p_E = 2E/L_d, \quad (93)$$

$$p_T = (N-1)k_B T/L_d. \quad (94)$$

The last two expressions, derived from a definition of the pressure in terms of mechanical quantities, may be compared with the formal definition of the pressure by means of partition functions. The equation corresponding to (93) is

$$p_E \approx \frac{N-1}{N-4} \frac{2E}{L_d} \quad (N \geq 5), \quad (95)$$

whereas (94) is also obtained from ensemble theory. This coincidence seems to be fortuitous in view of the difference between (93) and (95).

For the collision frequency the three lines of argument listed for the pressure lead to the following expressions:

$$v_{\{v_{i0}\}} = \frac{1}{NL_d} \sum_{i,j=1}^N |v_{i0} - v_{j0}|, \quad (96)$$

$$v_E = \frac{2(N-1)}{L_d} \frac{\Gamma(\frac{1}{2}(N-1))}{\Gamma(\frac{1}{2}N)} \sqrt{E/m}, \quad (97)$$

$$v_T = \frac{2(N-1)}{L_d} \sqrt{k_B T/m}. \quad (98)$$

The no-collision probability for a smallest stationary ensemble is found to be

$$W_{\{v_{i0}\}}(t) = (1/NL_d^{N-1}) \sum_{i=1}^N \left[\prod_{\substack{j=1 \\ j \neq i}}^N (L_d - |v_{i0} - v_{j0}| t)_+ \right] \quad (99)$$

where $(\dots)_+$ is defined by Eq. (67). Averaging the first polynomial defined by (99) over all velocities with $|V_0| = \sqrt{2E/m}$ one finds

$$W_E(t) = 1 - v_E t + O(t^2)$$

$$= \sum_{n=0}^{N-1} \alpha_n (-v_E t)^n \quad \text{for } v_E t < \frac{2\Gamma(\frac{1}{2}(N+1))}{\sqrt{\pi}\Gamma(\frac{1}{2}N)}, \quad (100)$$

$$\alpha_n = \frac{(N-1)!\Gamma(\frac{1}{2}(N-1))}{(N-1-n)!\Gamma(\frac{1}{2}(N-1-n))} \left[\frac{\Gamma(\frac{1}{2}N)}{2\Gamma(\frac{1}{2}(N+1))} \right]^n H_n, \quad (101)$$

$$H_n = \frac{1}{n! \sqrt{\pi}} \int dv [f(v)]^n \exp(-v^2), \quad (102)$$

$$f(v) = \frac{1}{\sqrt{2}} \int dw |v-w| \exp(-w^2)$$

$$= \sqrt{\pi/2} \left[v \operatorname{erf} v - \frac{1}{\sqrt{\pi}} \exp(-v^2) \right]. \quad (103)$$

H_n can be calculated analytically for $n=0, 1, 2$ but only numerically for $n \geq 3$. This has been done for $n \leq 80$ and these quantities were used to calculate $W_E(t)$ for $v_E t \leq 7$ and various values of N . Curves showing the probability W_E as function of the scaled time $v_E t$ are displayed in Fig. 15 for $N=2, 5, 10, 20, 40, \infty$. No closed expression for W_T can be derived from (100) to (103) but it can be shown that

$$\bar{W}_T(t) \leq W_T(t) \leq \frac{\Gamma(\frac{1}{2}(N-1))}{\gamma(\frac{1}{2}(N-1), mL_d^2/4t^2 k_B T)} \bar{W}_T(t), \quad (104)$$

where

$$\bar{W}_T(t) = \int_0^{mL_d^2/4t^2} dE h_T(E) W_E(t) \quad (105)$$

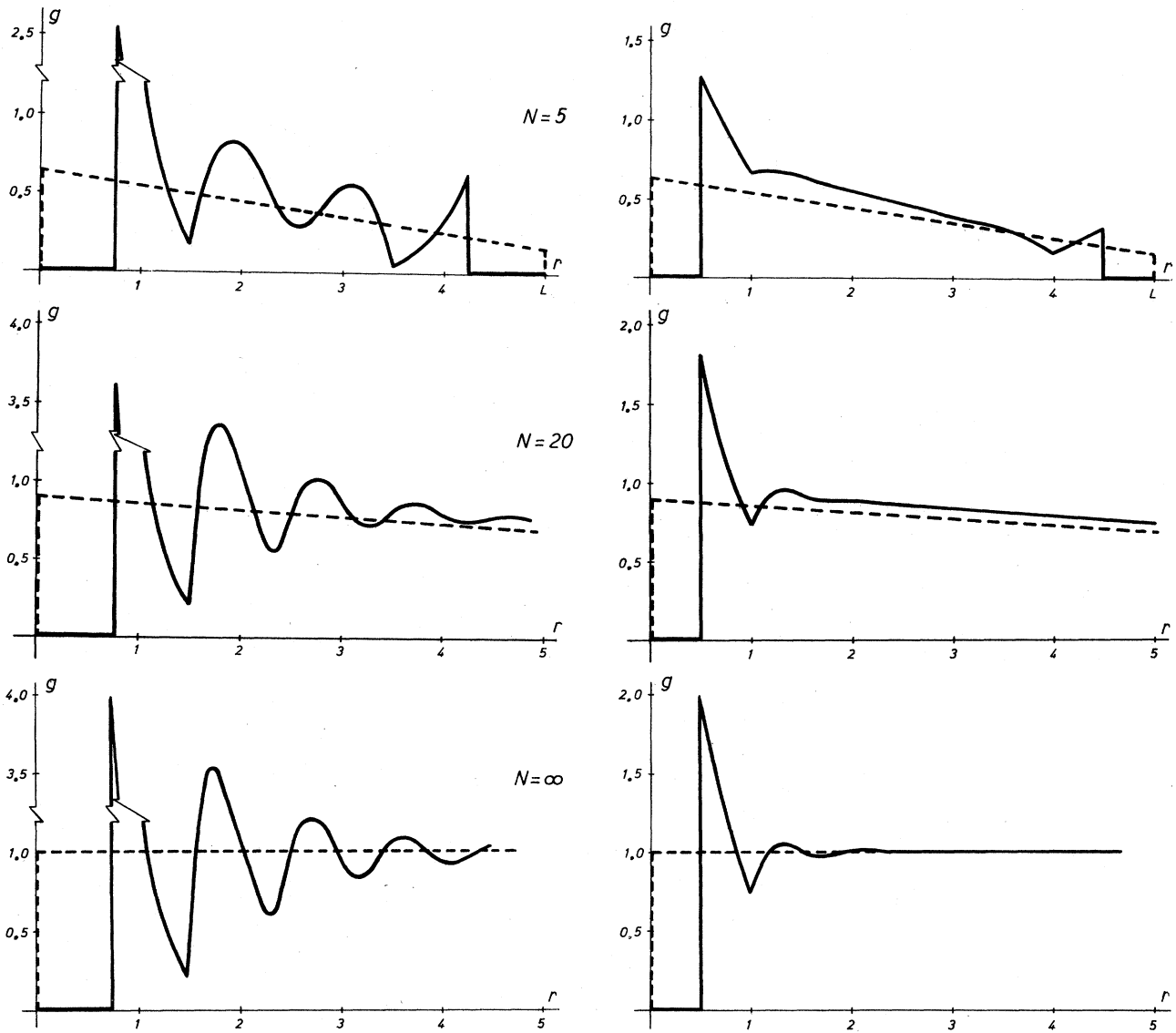


FIG. 14. Pair distribution function for $N=5, 20, \infty$ (solid line lhs $d=0.75/\rho$; solid line rhs $d=0.5/\rho$; dashed line $d=0$).

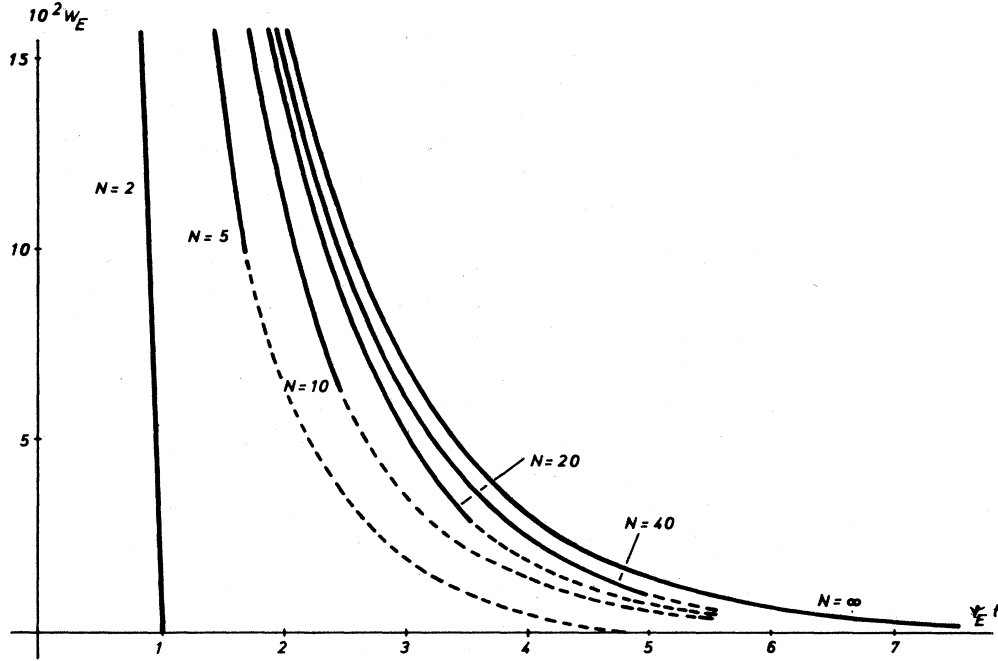
and $\gamma(a, x)$ is the incomplete γ function

$$\gamma(a, x) = \int_0^x dt t^{a-1} \exp(-t). \quad (106)$$

As before for $N=2$ and $N=3$ the velocity autocorrelation function is approached from two sides. For short

times the content of the intersections of a shifted simplex with its (unshifted) neighboring ones is calculated up to a given order of t . Since the calculations increase rapidly with the order, we stopped after the quadratic term of $\langle v_{i0} v_{1t} \rangle_{\{v_{i0}\}}$,

$$\begin{aligned} \langle v_{i0} v_{1t} \rangle_{\{v_{i0}\}} = & (1/N) \sum_{i,j=1}^N v_{i0}^2 - (t/2NL_d) \sum_{i,j=1}^N |v_{i0} - v_{j0}|^3 \\ & + (t^2/4NL_d^2) \sum_{i,j,k=1}^N [-(v_{i0} - v_{j0})^2 (v_{i0} - v_{k0})^2 + 3(v_{i0} - v_{j0}) |v_{i0} - v_{j0}| (v_{i0} - v_{k0}) |v_{i0} - v_{k0}|] \\ & + O(t^3) \text{ for } 2t^2 \sum_{i=1}^N v_{i0}^2 < L_d^2. \end{aligned} \quad (107)$$

FIG. 15. No-collision probability for $N=2,5,10,20,40, \infty$.

This may be integrated term by term to give the first polynomial of the VAF for the microcanonical ensemble which is in normalized form

$$\begin{aligned} \psi_E(t) &= \frac{mN}{2E} \langle v_{10} v_{1t} \rangle_E = 1 - \frac{8}{L_d} \frac{\Gamma(\frac{1}{2}(N+1))}{\Gamma(\frac{1}{2}N)} \sqrt{E/m\pi t} + 9\sqrt{3} \frac{(N-2)N}{(N+1)L_d^2} \frac{E}{m\pi} t^2 + O(t^3) \\ &= 1 - 2\nu_E t + O(t^2) \quad \text{for } 4Et^2 < mL_d^2. \end{aligned} \quad (108)$$

A comparison of ψ_E and ψ_T in the thermodynamic limit, discussed in the next section, led us to conjecture that the first polynomial for ψ_E is

$$\psi_E(t) = 1 + \sum_{n=1}^{N-1} \beta_n (-\nu_E t)^n \quad \text{for } \nu_E t < \frac{2\Gamma(\frac{1}{2}(N+1))}{\sqrt{\pi}\Gamma(\frac{1}{2}N)}, \quad (109)$$

$$\beta_n = \frac{N!}{2(N-1-n)!} \frac{\Gamma(\frac{1}{2}(N-1))}{\Gamma(\frac{1}{2}(N+1+n))} \left[\frac{\Gamma(\frac{1}{2}N)}{2\Gamma(\frac{1}{2}(N+1))} \right]^n I_n, \quad (110)$$

$$I_n = \frac{n+1}{\sqrt{\pi}} \int dv \exp(-v^2) \sum_l \frac{[f(v)]^{n-2l}}{(n-2l)!} \left[\frac{1}{4} g^2(v) \right]^l \frac{1}{(l!)^2}, \quad (111)$$

$$g^2(v) = f^2(v) - \frac{1}{2}\pi v^2, \quad (112)$$

$f(v)$ being given by (103). Using tabulated integrals³⁴ one can identify the first three terms of (109) and (108). We also found numerical agreement of (109) with a second representation of ψ_E , Eq. (117) below, for $N=3, \dots, 6$ so that we are quite sure that (109) to (112) gives the correct short-time behavior of the VAF ψ_E for finite N . Similar as for W_T before bounds of ψ_T can be derived from ψ_E , viz.,

$$\left| \frac{1}{2}(N-1)k_B T \psi_T(t) - \int_0^{mL_d^2/4t^2} dE h_T(E) E \psi_E(t) \right| \leq \int_{mL_d^2/4t^2}^{\infty} dE h_T(E) E. \quad (113)$$

The second approach is a series representation valid for arbitrary times. The generalization of (81) reads

$$\begin{aligned} \langle v_{10}v_{1t} \rangle_{\{v_{i0}\}} &= N^{-1} \beta^{2-2N} \sum_{A (\neq 0)} [\sin^2(\beta a_1)]^{N-1} \left[\prod_{k=1}^N a_k^{-2} \right] (A \cdot V'_0)^2 \exp(i\alpha A \cdot V'_0 t) \\ &= -\frac{\partial^2}{\partial(\alpha t)^2} N^{-1} \beta^{2-2N} \sum_{A (\neq 0)} [\sin^2(\beta a_1)]^{N-1} \left[\prod_{k=1}^N a_k^{-2} \right] \exp(i\alpha A \cdot V'_0 t); \end{aligned} \quad (114)$$

$$\alpha = 2\pi/L_d^2; \quad \beta = \pi/L_d; \quad A = (a_1, a_2, \dots, a_N), \quad Na_i/L_d = \text{integer}, \quad \sum_{i=1}^N a_i = 0. \quad (115)$$

Because $\{A\}$ is again the lattice reciprocal to $\{B\}$ it is evident from (114) that $\langle v_{10}v_{1t} \rangle_{\{v_{i0}\}}$ is almost periodic. If $(N-1)$ -dimensional polar coordinates are introduced the integration over all directions of V'_0 leads to tabulated integrals of trigonometric functions and integral representations of Bessel functions times powers.³⁴ Parametrizing the vectors A by $(N-1)$ -tuples

$$\underline{n} = (n_1, \dots, n_{N-1}), \quad n_k \text{ integer}, \quad (116)$$

one obtains

$$\begin{aligned} \psi_E(t) &= 2^{(N-3)/2} \Gamma(\frac{1}{2}(N-1)) \sum'_{\underline{n}} \left[\frac{1}{\pi} \sin \left[\frac{n\pi}{N} \right] \right]^{2N-2} \left[\prod_{k=1}^{N-1} \left[n_k - \frac{n}{N} \right]^{-2} \right] \\ &\quad \times [(z_{E,\underline{n}} t)^{(3-N)/2} J_{(N-3)/2}(z_{E,\underline{n}} t) - (N-2)(z_{E,\underline{n}} t)^{(1-N)/2} J_{(N-1)/2}(z_{E,\underline{n}} t)], \end{aligned} \quad (117)$$

$$\sum'_{\underline{n}} = \sum_{n_1, \dots, n_{N-1}} \text{ with } Nn_k \neq n, \quad (118)$$

$$n = n_1 + \dots + n_{N-1}, \quad (119)$$

$$z_{E,\underline{n}} = \frac{2\pi}{L_d} \sqrt{2E/m} \left[n_1 + \dots + n_{N-1} - \frac{n^2}{N} \right]^{1/2}. \quad (120)$$

This formula has been evaluated for small systems; the result is displayed in Fig. 13 for $N=3,4,5$. The infinite oscillations of $\langle v_{10}v_{1t} \rangle_{\{v_{i0}\}}$ still show up in the average ψ_E but the amplitude decreases, rather rapidly for larger N . For very large times only $2N(N-1)$ -tuples contribute essentially so that the asymptotic form of (117) is

$$\begin{aligned} \psi_E(t) &\sim -\frac{2^{N/2} N \Gamma(\frac{1}{2}(N-1))}{\sqrt{\pi(N-1)}} \left[\frac{N}{\pi} \sin \left[\frac{\pi}{N} \right] \right]^{2N-2} (z_E t)^{(2-N)/2} \sin \left[z_E t - \frac{N\pi}{4} \right], \\ z_E &= \frac{2\pi}{L_d} \left[\frac{2E(N-1)}{mN} \right]^{1/2}. \end{aligned} \quad (121)$$

This shows that the oscillations persist *ad infinitum* and the amplitude decreases finally as $t^{1-N/2}$. If the product of $\langle v_{10}v_{1t} \rangle_E$ and (89) is integrated one obtains a series representation of $\langle v_{10}v_{1t} \rangle_T$. Its normalized form is

$$\psi_T(t) = \frac{1}{N-1} \sum'_{\underline{n}} \left[\frac{1}{\pi} \sin \left[\frac{n\pi}{N} \right] \right]^{2N-2} \left[\prod_{k=1}^{N-1} \left[n_k - \frac{n}{N} \right]^{-2} \right] (1 - z_{T,\underline{n}}^2 t^2) \exp(-\frac{1}{2} z_{T,\underline{n}}^2 t^2), \quad (122)$$

$$z_{T,\underline{n}} = \frac{2\pi}{L_d} \sqrt{k_B T/m} \left[n_1^2 + \dots + n_{N-1}^2 - \frac{n^2}{N} \right]^{1/2}. \quad (123)$$

Curves of ψ_T as functions of $v_T t$ calculated by means of (122) are displayed in Fig. 6 for $N=2,4,6$. The asymptotic form of (122) corresponding to (121)

$$\psi_T(t) \sim \frac{2N}{(1+\delta_{N2})(N-1)^2} \left[\frac{N}{\pi} \sin \left[\frac{\pi}{N} \right] \right]^{2N-2} \left[1 - \frac{4\pi^2 k_B T (N-1) t^2}{m L_d^2 N} \right] \exp \left[-\frac{2\pi^2 k_B T (N-1) t^2}{m L_d^2 N} \right] \quad (124)$$

has already been derived by Evans;¹⁴ it is a good approximation to (122) if $t^2 \geq m L_d^2 N / 2\pi^2 k_B T (N-1)$.

VI. THERMODYNAMIC LIMITS

The results of the preceding section allows us to study in detail how the expectation values considered here

behave for increasing N if the densities

$$\rho = N/L = \rho_d(1+d\rho_d), \quad \rho_d = N/L_d = \rho/(1-d\rho), \quad (125)$$

the energy per particle,

$$\epsilon = E/N \text{ or } k_B T(N-1)/2N, \quad (126)$$

and all other parameters are either kept fixed (e.g., m, d) or restricted to finite domains (e.g., r, t). Of course the thermodynamic limit (TDL) makes sense only for expectation values $\langle \cdots \rangle_E$ and $\langle \cdots \rangle_T$ because an infinite set of parameters would be needed to specify the limit of $\langle \cdots \rangle_{\{v_{i0}\}}$. While the calculation of the limit $N \uparrow \infty$ may raise difficulties for some of the expectation values its meaning is quite clear: The TDL of such a quantity is an approximation to its true value for very large systems. If we use the term "infinite system" it is therefore always only in the sense of a "very large system" because a rigorous mathematical description of a truly infinite system calls for a mathematical framework wider than the one used here.^{35,22} Since we do not extend the concepts used up to now we cannot claim that the TDL of an expectation value represents a property of an infinite hard-rod system nor can we say anything about the ergodic properties of such systems. On the other hand, our statements on the equivalence of the time average and the average over certain parts of the energy surface, on the existence of recurrence times, and on the irreversible evolution of expectation values caused by a spread of the initial velocities, all remain valid no matter how large the system is. If the assertion merely states the existence of a property its form is independent of N . Differences between small and large systems can and do show up only if the statement can be strengthened to relate the property to quantities depending on the size of the system. Consider for instance the recurrence time: Such times exist for every system and all initial conditions, the shortest "period" being $L_d \sqrt{m/E}$. This value, obtained from setting $V'_0 t$ equal to one of the shortest lattice vectors $B \neq 0$, tends to infinity in the thermodynamic limit. From this one could conclude that, contrary to finite systems, the initial state of an infinite system is never realized again. However, a more thorough reasoning would be the following: If the observation time is restricted recurrences are found only for sufficiently small systems. If the systems become larger less and less recurrences are found in a given time interval until finally there are no recurrences any more once the systems have transcended a certain size. If on the other hand the size of the system is limited but not the observation time, any number of recurrences can be found for each of them. This example shows, as do two other examples discussed in the following, that apparent qualitative differences between finite and infinite systems may originate simply from performing two limits in different order.

The second example of this sort is the pair distribution function. The TDL of the polynomials (91) is the series

$$g(r) = \rho_d \sum_n \frac{1}{n!} \Theta(|r| - (n+1)d) \{ \rho_d [|r| - (n+1)d] \}^n \times \exp\{-\rho_d [|r| - (n+1)d]\}. \quad (127)$$

The function (127) reduces to the constant function $g(r) = \rho$ for $d=0$. In any case

$$\lim_{|r| \uparrow \infty} g(r) = \rho > 0, \quad (128)$$

whereas the lhs vanishes for every finite system. Equation (127) has been obtained by Zernike and Prins¹⁶ already in 1927; the first formal derivation seems to be due to Salsburg *et al.*²⁵ The function (127) may also be obtained as TDL of the two-particle distribution function $D_2(x, y)$ of Leff and Coopersmith.¹² These authors considered systems with fixed walls while we enclosed the particles in a movable box. That the TDL is the same for two different models is not surprising but these calculations show explicitly that boundary conditions become more and more irrelevant as the size of the system increases. The pair distribution function (127) is displayed in Fig. 14 for $\rho=1$ and two values of d . Comparison with the five-particle system shows that the influence of increasing diameter d is already clearly perceivable in the small system. The TDL and the function for the finite system have been found to agree up to a few percent within the range of the first three neighbors ($\rho |r| < 3$) for systems with only 20 particles.

A similar "rapid" convergence toward the TDL is also found for the pressure and the collision frequency. The limits of these quantities are

$$p_{\infty, \epsilon} = 2\rho_d \epsilon, \quad (129)$$

$$p_{\infty, T} = \rho_d k_B T, \quad (130)$$

$$v_{\infty, \epsilon} = 2\rho_d \sqrt{2\epsilon/m\pi}, \quad (131)$$

$$v_{\infty, T} = 2\rho_d \sqrt{k_B T/m\pi}. \quad (132)$$

If one puts

$$\gamma = m/4\epsilon \text{ or } m/2k_B T \quad (133)$$

the pressure and the collision frequency may be represented by the integrals

$$p_{\infty, \epsilon} = \sqrt{\gamma/\pi} \int dv \exp(-\gamma v^2) p_\gamma(v), \quad (134)$$

$$p_\gamma(v) = \sqrt{\gamma/\pi} \int dw \exp(-\gamma w^2) \left[\frac{1}{2} m \rho_d (v-w)^2 \right] \\ = \frac{1}{2} m \rho_d (v^2 + \frac{1}{2} \gamma^{-1}); \quad (135)$$

$$v_{\infty, \gamma} = \sqrt{\gamma/\pi} \int dv \exp(-\gamma v^2) v_\gamma(v), \quad (136)$$

$$v_\gamma(v) = \sqrt{\gamma/\pi} \int dw \exp(-\gamma w^2) \rho_d |v-w| \\ = \rho_d \left[v \operatorname{erf}(v\sqrt{\gamma}) + \frac{1}{\sqrt{\gamma\pi}} \exp(-\gamma v^2) \right]. \quad (137)$$

These integral representations are not chosen at random but emerge quite naturally if one passes directly from the expectation value for a smallest stationary ensemble to that for a canonical one ($N < \infty$). Comparison of (134) and (135) with (92) suggests the interpretation of $p_\gamma(v)$ as the pressure acting on a particle with random position and definite velocity v moving in an infinite system of hard rods with random positions and Maxwellian velocity distributions. Likewise, $v_\gamma(v)$ may be viewed as the collision frequency of such a particle [cf. Eqs. (136), (137), and (96)] which agrees with the interpretation of the function (137) as proposed by Lebowitz and Percus.¹⁷

A similar integral representation is found for the no-

collision probability $W_{\infty,\gamma}(t)$. To see how this probability is related to that for the finite system, consider first $W_E(t)$ for $N < \infty$. This function is represented by a series of polynomials each valid in a certain part of the domain. As N goes to infinity the polynomials become series but only the first one survives because the time where the first polynomial fails to represent $W_E(t)$ tends to infinity as \sqrt{N} . For $N \uparrow \infty$ and $\gamma = m/4\epsilon$ one obtains from (100)

$$W_{\infty,\gamma}(t) = \sum_{n=0}^{\infty} H_n(-v_{\infty,\gamma}t)^n \quad (138)$$

If one puts $\gamma = m/2kT$ the series (138) is also the TDL of $W_T(t)$ because $\gamma(a, \infty) = \Gamma(a)$ and the bounds in (104) converge. Looking at the definition of H_n by integrals, Eqs. (102) and (103), one sees that the collision probability may be written as

$$W_{\infty,\gamma}(t) = \sqrt{\gamma/\pi} \int dv \exp(-\gamma v^2) W_{\infty,\gamma}(v,t), \quad (139)$$

$$W_{\infty,\gamma}(v,t) = \exp[-v_{\gamma}(v)t] \quad (140)$$

Following Lebowitz and Percus¹⁷ and Levitt¹⁹ $W_{\infty,\gamma}(v,t)$ may be interpreted as the no-collision probability of a particle with velocity v and random position which is surrounded by infinitely many other particles with random positions and Maxwellian velocity distributions. However, there is a difference to be noted between the velocity dependent quantities $p_{\gamma}(v)$, $v_{\gamma}(v)$, and the function $W_{\infty,\gamma}(v,t)$: While the former appear also for finite systems, if the center of mass is allowed to move, it is not the function (140) but the function

$$W_{N,\gamma}(v,t) = \left[e_{N,\gamma}(v,t) - \frac{1}{N} \tilde{v}_{N,\gamma}(v,t)t \right]^{N-1}, \quad (141)$$

$$\psi_{\infty,\gamma}(t) = \sqrt{\gamma/\pi} \int dv \exp[-\gamma v^2 - v_{\gamma}(v)t] \{ [1 - v_{\gamma}(v)t] I_0([v_{\gamma}^2(v) - \rho_d^2 v^2]^{1/2}t) + [v_{\gamma}^2(v) - \rho_d^2 v^2]^{1/2} t I_1([v_{\gamma}^2(v) - \rho_d^2 v^2]^{1/2}t) \}, \quad (144)$$

where $I_{0,1}$ are modified Bessel functions. This form of the VAF has first been obtained by Lebowitz and Percus.¹⁷ The asymptotic form of $\psi_{\infty,\gamma}(t)$ for large t extracted from (144) is

$$\begin{aligned} \psi_{\infty,\gamma}(t) \sim & -2\sqrt{2}(2\pi - 5)(\pi v_{\infty,\gamma}t)^{-3} \\ & -24(3\pi - 8)(\pi v_{\infty,\gamma}t)^{-4} \\ & -2\sqrt{2}(36\pi^2 + 72\pi - 461)(\pi v_{\infty,\gamma}t)^{-5} - \dots \end{aligned} \quad (145)$$

The leading term has already been found by Jepsen.¹⁵

Similar to the no-collision probability the series (143) is also the TDL of $\psi_T(t)$ as can be concluded from the estimate (113). That ψ_E and ψ_T both approach the same function in the TDL is expected on general grounds but not obvious from the form of these functions for small

$$\begin{aligned} e_{N,\gamma}(v,t) = & \frac{1}{2} \{ \operatorname{erf}[\sqrt{\gamma}(v + N/\rho_d t)] \\ & - \operatorname{erf}[\sqrt{\gamma}(v - N/\rho_d t)] \}, \\ \tilde{v}_{N,\gamma}(v,t) = & \sqrt{\gamma/\pi} \int_{v-(N/\rho_d t)}^{v+(N/\rho_d t)} dw \exp(-\gamma w^2) \rho_d |v-w|, \end{aligned} \quad (142)$$

which appears in (139) in this case. The simplification in the dynamics of very large systems mentioned in Sec. II consists in replacing Eqs. (141), (142) by Eqs. (140), (137). Comparing the TDL of $W_E(t)$ with the corresponding functions for finite systems one sees that the convergence is rather slow, especially if times are considered where a few collisions are expected to take place ($v_E t \leq 5$). Inspection of Fig. 15 indicates that a system with about 20 particles, which up to now seemed to approximate an "infinite" system very well, cannot be considered as typical if time-dependent phenomena are studied. The formal reason for this insufficiency can be understood from the series representations (138) and (100). As the observation time increases more and more terms contribute essentially to $W_E(t)$, but the higher the power of t the more the expansion coefficient deviates from its TDL. Physically the discrepancy originates from the following fact: The larger the system is the better is the chance that the tagged particle is initially rather isolated, i.e., far away from its next neighbors.

A similar slow convergence toward the TDL is found for the velocity autocorrelation function, the last of the quantities considered here. The first polynomial of $\psi_E(t)$, Eq. (109), tends toward the series

$$\psi_{\infty,\gamma}(t) = \sum_{n=0}^{\infty} I_n(-v_{\infty,\gamma}t)^n \quad (143)$$

with $\gamma = m/4\epsilon$ and its range extends to infinity. The series representation (143) is equivalent to the integral representation

systems. The only thing one can guess from looking at Figs. 6 and 13 is that agreement can be found mostly in the beginning, i.e., for times bounded by the second zero of ψ_E . This region has to become larger and larger as N increases because the asymptotic forms of ψ_E and ψ_T have already been found to be completely different for every finite system [cf. Eqs. (121) and (124)]. It is also clear that the inverse power law for the infinite system, Eq. (145), originates from the short-time behavior of large but finite systems. To see this in more detail one can try to evaluate (109) for larger and larger N . However, this is limited by the accuracy which can be obtained in calculating the coefficients of the power series and by the magnitude and number of terms that have to be taken into account in this alternating series. These considerations limited the evaluation of (109) to $N \leq 40$. For these numbers of particles the first polynomial represents ψ_E not far beyond the first minimum so that the series (109) is only

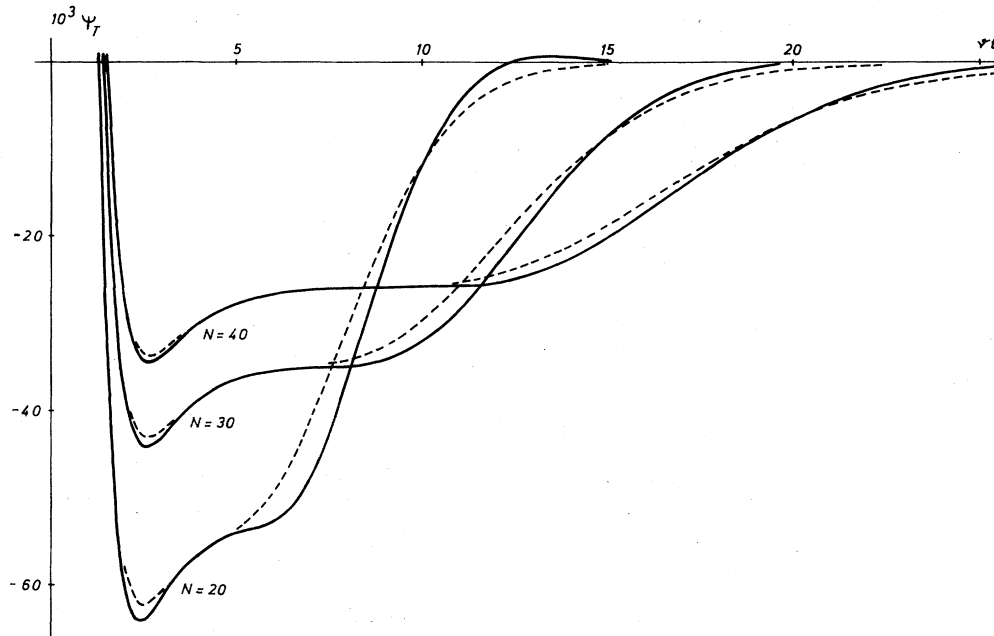


FIG. 16. Velocity autocorrelation functions ψ_E (solid line) and ψ_T (dashed line) for $N=20,30,40$.

suites to show how the deep minima found for small systems approach the flat minimum of the TDL, but not to tell us how the oscillating tail disappears with increasing N . It is, however, possible to continue the curves of ψ_E by means of the series (117) which for $N \leq 40$ fortunately converges fast enough for times outside the domain of the first polynomial. The resulting curves, displayed for $N=20,30,40$ in Fig. 16, have a common feature which hardly could have been expected from inspection of the curves for small systems (Fig. 13). For $N > 15$ there appears a small shoulder after the first minimum which, as

N increases, develops more and more into a horizontal plateau between the first minimum and the second zero. The length of this plateau increases with N while its depth below zero is approximately proportional to $1/N$. It is interesting to note that similar plateaus appear for the systems studied by Lebowitz and Sykes¹³ but their depth is only $1/2N$ and both their beginnings and ends tend toward infinity as N increases.

To come closer to the thermodynamic limit still larger systems have to be considered. This is only possible for ψ_T but we know already from (113) that this function ap-

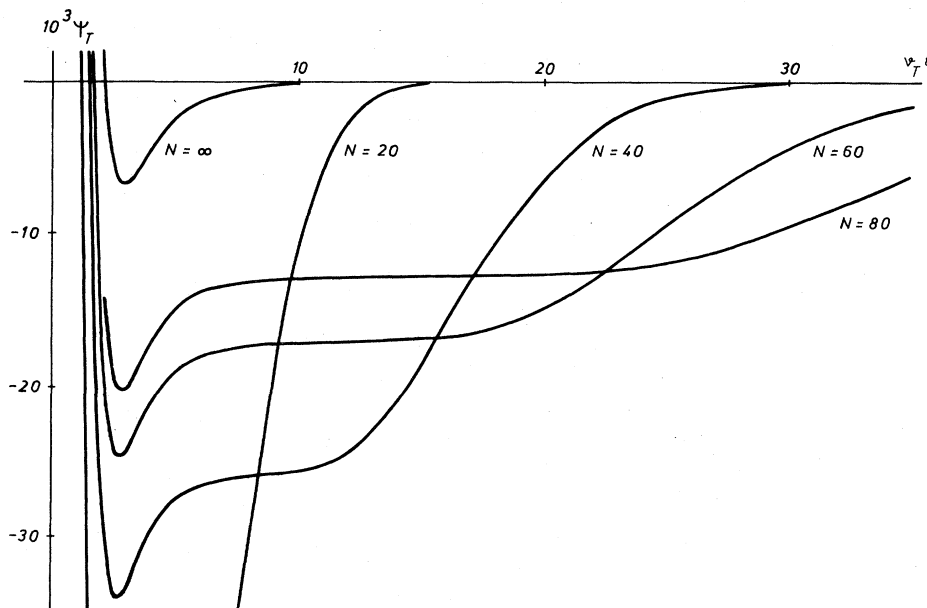


FIG. 17. Velocity autocorrelation function ψ_T for $N=20,40,60,80, \infty$.

proaches the same limit as ψ_E . Moreover, if $N \geq 20$ ψ_E does not differ much from ψ_T in the region of interest as can be seen from Fig. 16. A formula suited for numerical evaluation for $N \leq 100$ is obtained by transforming (122) in the following form:

$$\psi_T(t) = \Phi(v_T t) + t \frac{\partial}{\partial t} \Phi(v_T t), \quad (146)$$

$$\Phi(\tau) = \frac{1}{(N-1)2\pi} \times \int_{-\pi}^{\pi} d\xi \sum_{p=1}^{N-1} \left[\frac{1}{\pi} \sin \left[\pi \frac{p}{N} \right] \right]^{2N-2} S_2 \left[\xi, \eta, \frac{p}{N} \right] \times S_3^{N-1} \left[\xi, \eta, \frac{p}{N} \right], \quad (147)$$

$$S_2(\xi, \eta, \lambda) = \sum_n \exp[-\eta(n+\lambda)^2 + i\xi(n+\lambda)], \quad (148)$$

$$S_3(\xi, \eta, \lambda) = \sum_n (n+\lambda)^{-2} \exp[-\eta(n+\lambda)^2 + i\xi(n+\lambda)], \quad (149)$$

$$\eta = \pi^3 \tau^2 / 2(N-1)^2. \quad (150)$$

The curves calculated by means of (146)–(150) for $N=20,40,60,80$ confirm the features found for ψ_E for $N=20,30,40$. The approach to the TDL is now evident from Fig. 17 and it can be rigorously proved that (146) tends to (144) for $N \uparrow \infty$. Having obtained this result and proven the coincidence of ψ_T and ψ_E in the TDL we used the series expansion of the modified Bessel functions to obtain the power-series representation (143). This series and some other results for finite systems then helped us to guess the general form of the first polynomial of ψ_E for $N < \infty$ [Eqs. (109)–(112)].

The discussion of the TDL of the VAF shows once more that qualitative differences between finite and infinite systems originate from different orders of limits, here $N \uparrow \infty$ and $t \uparrow \infty$. It is also evident from Fig. 17 that only rather large systems ($N \simeq 100$) are representative for the TDL of the VAF.

VII. CONCLUSION AND OUTLOOK

For the one-dimensional N -particle system described in Sec. II some principal questions could be clarified. Our discussion of time and ensemble averages, recurrence times, and approach to equilibrium, is in some respect more general than the results found in literature. We also obtained exact expressions for a number of expectation values. Five phase-space functions representing typical properties of the system (pair distribution function, pressure, collision frequency, no-collision probability, velocity autocorrelation function) were considered and the average performed over three ensembles which are of general interest: canonical, microcanonical, and smallest stationary ensemble (equal to time average).

We were especially interested to see how these quantities calculated for finite systems change with the size of the system (thermodynamic limit). For quantities depending on the state of the system at one instant only (pair dis-

tribution function) or on a pair of instants differing by an infinitesimal amount (pressure, collision frequency) the results obtained for small systems agreed qualitatively with those for large ones and we observed a rapid convergence toward the thermodynamic limit. If on the contrary the quantity depends on more instants separated by finite time intervals (no-collision probability, velocity autocorrelation function) the convergence toward the thermodynamic limit turned out to be very slow and the behavior of small systems was found to be atypical for the thermodynamic limit. If this is a general feature (which should be tested by further examples) this is certainly of some interest for extrapolating the results of computer experiments which are necessarily performed with a limited number of particles.

It is natural to ask whether the present model and the methods used here can be varied or generalized. First we want to point out that the reflection trick works equally well for systems with fixed walls. We found good agreement between the velocity autocorrelation function for $N=4,6$ and movable walls (ring system) and the VAF for $N=2,3$ for fixed walls, but the latter functions were much more tedious to compute. This inconvenient feature may be traced to the fact that the fixed wall system does not possess the cyclic symmetry of the ring system which helped us to simplify most results considerably. While we cannot expect drastic deviations from the results obtained here by merely changing the boundary conditions, essential differences are to be expected for more drastic changes of the underlying dynamics. One possibility, already considered for the infinite system,^{36,37} is to pass from the deterministic model to a stochastic one by assuming that the colliding particles can pass through each other with a certain probability. Another possibility is to study the quantum mechanics of hard-rod systems. This has already been done by Born⁶ and Deutch *et al.*⁷ for one particle between fixed walls which corresponds to our system with $N=2$. More interesting than these two variations, which are in part the subject of current research, are certainly extensions to more dimensions and various shapes of the container. However, if we try to generalize the techniques used here to such problems we are faced with two difficulties. The first one can be understood by considering the motion of a point inside a hexagon, which arises if one studies the relative motion of three-point particles in a massless cubic box which is allowed to move without rotations. In this model the true path of the point within the hexagon may be unfolded into a straight line by successive reflections of hexagons along their boundaries but contrary to what has been found here these reflections are not uniquely determined by the position of the last hexagon only. Thus although the true path is completely fixed by the straight line it is not as easy as it was here to recover the true position and velocity of the point from a given ray. The second difficulty is even more serious. If the particles have finite extent there appear forbidden regions within the configuration space corresponding to situations where two or more particles would overlap. The simplest example of this sort is a point moving between two concentric squares; this can be interpreted as relative motion of two hard squares en-

closed by a massless, freely movable square box. If the reflection trick is applied to the outer square one obtains a lattice of small squares which act onto the representative point like impenetrable obstacles. As time evolves this point is therefore scattered again and again, and this in a very chaotic way since the scatterers all have convex corners and a small change of position or velocity before a scattering process can result in large differences afterwards. Richens and Berry³⁸ have shown that both difficulties mentioned here are related and typical for pseudointegrable systems. We therefore conclude that general-

izations to higher dimensions are by no means straightforward if possible at all.

ACKNOWLEDGMENTS

We thank O. J. Eder, T. Lackner, and M. Posch for stimulating discussions, the latter also for assistance in some of the numerical calculations. One of us (J.R.) acknowledges financial support by the Austrian Research Center, Seibersdorf.

-
- ¹H. L. Frisch, *Phys. Rev.* **104**, 1 (1956).
²H. L. Frisch, *Phys. Rev.* **109**, 22 (1958).
³D. W. Jepsen, *J. Math. Phys.* **6**, 407 (1965).
⁴Ei. Teramoto and Ch. Suzuki, *Prog. Theor. Phys.* **14**, 412 (1955).
⁵J. L. Lebowitz and J. K. Percus, *Phys. Rev.* **155**, 123 (1967).
⁶M. Born, *K. Dan Vidensk. Selsk. Mat. Fys. Medd.* **30**, No. 2 (1955).
⁷J. M. Deutch, J. L. Kinsey, and R. Silbey, *J. Chem. Phys.* **53**, 1047 (1970).
⁸Ei. Teramoto and Ch. Suzuki, *Prog. Theor. Phys.* **14**, 411 (1955).
⁹R. Nossal, *J. Math. Phys.* **6**, 193 (1965).
¹⁰A. Hobson and D. N. Loomis, *Phys. Rev.* **173**, 285 (1968).
¹¹L. Tonks, *Phys. Rev.* **50**, 955 (1936).
¹²H. S. Leff and M. H. Coopersmith, *J. Math. Phys.* **8**, 306 (1967).
¹³J. L. Lebowitz and J. Sykes, *J. Stat. Phys.* **6**, 157 (1972).
¹⁴J. W. Evans, *Physica* **95A**, 225 (1979).
¹⁵D. W. Jepsen, *J. Math. Phys.* **6**, 405 (1965).
¹⁶F. Zernike and J. A. Prins, *Z. Phys.* **41**, 184 (1972).
¹⁷J. L. Lebowitz and J. K. Percus, *Phys. Rev.* **155**, 122 (1967).
¹⁸J. L. Lebowitz, J. K. Percus, and J. Sykes, *Phys. Rev.* **171**, 224 (1968).
¹⁹D. G. Levitt, *J. Stat. Phys.* **7**, 329 (1973).
²⁰J. K. Percus, *Phys. Rev. A* **9**, 557 (1984).
²¹M. Aizenman, S. Goldstein, and J. L. Lebowitz, *Commun. Math. Phys.* **39**, 289 (1975).
²²M. Aizenman, J. L. Lebowitz, and J. Marro, *J. Stat. Phys.* **18**, 179 (1978).
²³J. L. Lebowitz and O. Penrose, *Phys. Today* **23** (2), 26 (1973).
²⁴J. Frenkel, *Kinetic Theory of Liquids* (Oxford University, New York, 1940), p. 126.
²⁵Z. W. Salsburg, R. W. Zwanzig, and J. G. Kirkwood, *J. Chem. Phys.* **21**, 1098 (1953).
²⁶R. Carmona and L. Gottdiener, *Kinam (Mexico)* **2**, 297 (1980).
²⁷K. Ikeda and T. Takano, *Prog. Theor. Phys.* **65**, 1542 (1981).
²⁸A. Hobson, *J. Math. Phys.* **16**, 2210 (1975).
²⁹H. Weyl, *Math. Ann.* **77**, 313 (1916).
³⁰E. Hlawka, *Theorie der Gleichverteilung* (BI Hochschultaschenbücher, Mannheim, 1979).
³¹W. Maak, *Fastperiodische Funktionen* (Springer, Berlin, 1967).
³²V. I. Arnold, *Mathematical Methods of Classical Mechanics* (Springer, New York, 1978).
³³M. V. Berry, in *Topics in Nonlinear Dynamics (La Jolla Institute)*, Proceedings of the Workshop on Topics in Nonlinear Dynamics (American Institute of Physics, New York, 1978), Vol. 46, p. 16.
³⁴I. S. Gradshteyn and I. M. Ryzhik, *Table of Integrals, Series, and Products* (Academic, New York, 1965).
³⁵E. Presutti, M. Pulvirenti, and B. Tirozzi, *Commun. Math. Phys.* **47**, 87 (1976).
³⁶G. R. Anstis, H. S. Green, and D. K. Hoffman, *J. Math. Phys.* **14**, 1437 (1973).
³⁷C. Kipnis, J. L. Lebowitz, E. Presutti, and H. Spohn, *J. Stat. Phys.* **13**, 107 (1983).
³⁸P. J. Richens and M. V. Berry, *Physica D* **2**, 495 (1981).